8-2-2019

Long-term performance of sustainable pavements using ternary blended concrete with recycled aggregates

Seth M. Wagner
Rowan University

LONG-TERM PERFORMANCE OF SUSTAINABLE PAVEMENTS USING TERNARY BLENDED CONCRETE WITH RECYCLED AGGREGATES

by

Seth M. Wagner

A Thesis

Submitted to the
Department of Civil and Environmental Engineering
College of Engineering
In partial fulfillment of the requirement
For the degree of
Master of Science in Civil Engineering
at
Rowan University
August 1, 2019

Thesis Advisor: Gilson R. Lomboy, D.Eng., Ph.D.

Acknowledgements

I would like to thank my advisor Dr. Gilson R. Lomboy for guiding this research and teaching me the difference between data and "good" data. I also thank my research committee members Dr. Douglas B. Cleary, D. Eng., Ph.D. and Dr. Yusuf A. Mehta, D. Eng., Ph. D. for always providing assistance when it was needed.

I would like to express gratitude to my parents Lon E. Wagner and Kathleen L. Weise for supporting me on this journey. I would not have made it this far without you.

Abstract

Seth M. Wagner
LONG-TERM PERFORMANCE OF SUSTAINABLE PAVEMENTS USING TERNARY BLENDED CONCRETE WITH RECYCLED AGGREGATES
2018-2019
Gilson R. Lomboy, D.Eng., Ph.D.
Master of Science in Civil Engineering

The purposes of this study were to (a) design concrete pavement mixtures with recycled concrete aggregates using ternary blends of cementitious materials and a low water-to-binder ratio, (b) measure the fresh and hardened properties of the proposed concrete mixtures and (c) assess the long-term performance of the concrete implementing the use of recycled coarse aggregates. Preliminary investigation into ternary blend combinations via the compressive testing of mortar cubes and isothermal calorimetry was used to predict an optimal blend of cementitious material. Mixes using recycled concrete aggregates at varying replacement rates were tested for fresh and hardened properties using the proposed blend. It was found that a blend of portland cement, Class C fly ash, and ground granulated blast furnace slag produced the highest strength of ternary binder. Ternary blended cement mixtures showed improvement in hardened properties in late-age testing. At 50% replacement of virgin aggregates, specimens showed comparable mechanical performance to the control mix.

Table of Contents

Table of Contents (Continued)

List of Figures

List of Figures (Continued)

Figure Page

List of Tables

Chapter 1

Introduction

Due to the high production rate of portland cement concrete, demand for suitable aggregates and portland cement raises concerns for both the environmental and economic availability of these materials. The production of portland cement and aggregates plays a large role in the creation of pollution in the concrete industry and depletes natural rock quarries. For many years, alternative materials have been used to either supplement or replace these in concrete materials to varying degrees of success.

Supplementary cementitious materials (SCM) are mineral admixtures – often byproducts of other industries – which can be used in combination with portland cement to improve the fresh and hardened properties of concrete. These admixtures can be hydraulic, exhibiting cementitious properties when reacted with water. They may also be pozzolanic, reacting with calcium hydroxide and water to provide additional strength. Common SCM include ground granulated blast furnace slag, fly ash and silica fume. Blast furnace slag is a byproduct of iron production, fly ash is produced from coal burning operations and silica fume is a byproduct of silicon and ferrosilicon alloy production. In locations where these industrial processes create an excess of these byproducts, it is possible to reduce both the environmental impact and cost of concrete construction with their use. Ternary blended binders consisting of two SCM and portland cement are actively researched for their additive benefits to concrete mixtures. In these cases, cementitious or pozzolanic mineral admixtures which are observed to have a positive interaction may be used to replace a significant portion of portland cement in a proposed binder.

Recycled concrete aggregate (RCA) or crushed concrete coarse aggregate (CCCA) is existing concrete which has been removed, crushed, and graded to be used as aggregate [1]. RCA consists of virgin aggregate (VA) coated fully or partially by hardened mortar from the previous mix. RCA tend to have higher porosity and poorer mechanical properties than virgin aggregates due to the presence of adhered mortar, which may be less hard or durable than rock. However, given appropriate constraints on usability, RCA may replace part or all of the required aggregates in a concrete mixture. In these cases, the demand for virgin aggregates may be reduced, preserving existing quarries. RCA may also be more readily available in some instances via on-site or local crushing facilities, reducing materials and transportation costs.

There is little in the way of literature addressing the use of ternary blended cements in conjunction with RCA replacement in concrete mixes. The purpose of this research is to perform additional experimentation on the interaction of ternary blended binders and crushed concrete coarse aggregates in developed concrete mixtures with low water-to-binder ratio. This work is divided into two tasks; (a) to determine an optimal ternary blended binder consisting of portland cement and two of: blast furnace slag, Class C fly ash, Class F fly ash and silica fume and (b) to assess the performance of concrete mixtures with varying amounts of recycled coarse aggregate and the effect of using a ternary blended binder in concrete mixtures with high RCA replacement rates.

Chapter 2

Literature Review

Recycled Concrete Aggregate (RCA)

Hardened concrete may be broken down and used as coarse aggregate for new mixes. Aggregate created by this recycling process is known as recycled concrete aggregate or crushed concrete coarse aggregate. Concrete is commonly recycled in this manner from the demolition of buildings and pavements [1]. Apart from impurities that may be present in aggregate of this type due to the wide variety of sources, the presence of mortar alters physical properties of the aggregate. Density is decreased, and porosity and adsorption are increased with respect to VA [2]. RCA is primarily used in consideration of the environmental impacts of concrete construction. The use of RCA prevents material from occupying landfills and limits the harvesting of virgin aggregates [3]. Depending on the cost and availability of VA, using RCA may also prove to be an economical choice where there is less cost in recycling than in removing and disposing of rubble, particularly in cases where a mobile recycling operation can be brought on to the site [4].

The production of RCA begins with demolition of the site. ACI Committee 555 provides a list of common types of structures that may be a part of this process [1]. These include mass concrete structures, underground concrete structures, reinforced concrete structures and prestressed/post-tensioned concrete structures. Different types of structures require additional considerations in demolition to avoid accidental collapse. Demolition methods are selected based on safety, environmental impact, budgetary constraints, and the size and location of the site. Available methods of demolition include: hand tools,

vehicle-mounted equipment, explosive blasting, chemical demolition agents, mechanical splitters, heat demolition and hydrodemolition.

Following successful demolition, reinforcement is removed from the debris, and the concrete is transported to a processing plant. Once at the plant, large rubble is crushed to suitable size via several differently-sized crushers. Aggregate size is reduced to a final maximum diameter of 20 to 25 millimeters [1]. Further processing is required to remove other contaminants in the concrete, which can vary by source. Any additional rebar in the concrete is removed by magnet. Other contaminants present in concrete removed from building demolitions include wood, plaster, plastic, oil, etc. ACI Committee 555 closely relates the operations at RCA processing plants to those of plants that process unused virgin aggregate.

American Concrete Pavement Association (ACPA) has found RCA stockpiles are notably more alkaline as a result of calcium hydroxide being leached from the pile [5]. The calcium hydroxide reacts with carbon dioxide to form carbonates. Abbaspour, et al. confirms these findings, noting increases in pH with stockpile aging as well as an increase in carbonate content [6]. ACPA suggests stockpiling washed RCA to help avoid carbonate runoff from clogging drains. Additionally, the acidity of rain reacting to form the carbonates may reduce or potentially neutralize the alkalinity of the stockpile [7]. There are no further known disadvantages to stockpiling RCA as opposed to virgin aggregate.

Production of crushed concrete coarse aggregate as an alternative source of coarse aggregate has a few notable environmental effects. Sources of virgin aggregate are finite in supply and ever reducing, and recycling already-used materials helps to preserve these

supplies [4]. In addition, reusing demolished concrete as RCA reduces the output of material from the construction industry into landfills. By processing RCA for a given project, the carbon dioxide emissions and energy consumption associated with quarrying can be reduced or eliminated [3]. RCA production can be accomplished via mobile recycling operations placed on the construction site or fixed recycling plants that require materials transportation off-site [8]. McIntyre, et al. conducted a study through which the optimal amount of RCA production was found to depend on both cement consumption and transportation [8]. If increasing the RCA replacement rate of a mix requires more cement to be added to maintain a target strength, RCA replacement begins to lose value. On-site recycling reduces the costs associated with materials transportation. McGinnis, et al. quantified the land use, water use, energy demand, and carbon emissions associated with the production of natural and recycled aggregates via field study [9]. Their study found that in all four categories, recycled aggregate production required a fraction of the resources of virgin aggregate production. The study concluded that RCA production had a 55% reduced environmental impact over virgin aggregate. Additionally, the study investigated the economic possibilities of RCA and found that recycled aggregates cost 74% of the price virgin aggregates between nearest competitors.

Aggregate Properties. The increase in aggregate void space in RCA greatly impacts the bulk density of the aggregates [10]. This is found via ASTM C29/C29M standard testing. Bulk density is essential for proportioning, voids calculation and volume control. A low percentage of voids in RCA is preferable for concrete production because less paste is required for mixing. Adding binder increases the cost of portland cement concrete. The presence of old, porous mortar adhered to recycled aggregates and the additional interfacial zones reduce the density of concrete with RCA. Specific gravity for recycled aggregate ranges from 2.2 to 2.6, lower than virgin aggregate which has a range of 2.4 to 2.9 [11-14].

Absorption, porosity and permeability are affected by the pore volume in the aggregate and between aggregates. These voids affect the strength, abrasion resistance and freeze-thaw durability of a concrete mixture. Porosity is the ratio of the voids in an aggregate to the total volume of the aggregate, and is found via ASTM C29/29M [15]. Porosity is higher in RCA than in virgin aggregates due to the adhered mortar content of recycled aggregates. Concrete mixtures using RCA thus require more water to maintain workability, and may suffer a decrease in hardened strength and density.

The Los Angeles (LA) Abrasion Test measures the effect of degradation on an aggregate while enduring impact, abrasion and grinding [16]. ASTM C131/131M-14 outlines this process. The aggregate sample is placed in a steel drum containing steel spheres, which undergoes a specified number of revolutions. A higher percent loss of aggregate mass following the test procedure indicates less resistance to crushing while a load is applied. Virgin aggregates tend to have a loss value between 10-20%, while RCA typically suffers 20-45% mass loss due to the removal of the adhered paste [11, 17].

ASTM C136/136M-14 details the process by which the particles size distribution of fine and coarse aggregates in a sample is determined [18]. Coarse aggregates are defined as those retained on a 4.75-mm opening sieve whereas fine aggregates pass through. The particle size distribution of aggregates is important to the construction process in engineering. Fine aggregates are stronger when placed under load and have less pore space. Using more coarse aggregate reduces construction cost as less binder is required to cover the surface area of the aggregates. Therefore, a gradation with an appropriate blend of fine and coarse aggregates (well-graded) is required to balance concrete strength with cost. A well-graded aggregate will result in small, tightly packed voids and a stable matrix structure. Fineness modulus (FM), which is used in portland cement concrete mixture design and quality control checks during concrete production, is also determined from fine aggregate gradation. Typical values of FM for fine aggregates are between 2.3 and 3.1.

The flat and elongated test determines the shape of aggregates to be used in a mixture. ASTM D4791–10 gives the process by which the percentage of elongated particles, flat particles, or flat and elongated particles is found for an aggregate sample [19]. Flat or elongated particles have a greater chance to fracture and are harder to compact. The shape for typical virgin aggregates is blended between well rounded smooth gravel, and angular rough crushed rock. RCA tends to be rougher due to the presence of adhered mortar [20]. The shape, texture and angularity of aggregates determine the uncompacted void content percentage. If the void content increases, it may be attributed to a greater angularity, less sphericity or a rougher surface of the aggregate. Angular aggregates create void space as angularity prohibits tight compaction [20].

Angular aggregates also require more binder material and subsequently increase mixture cost. Angular aggregates improve interlocking within the concrete matrix, increasing compressive strength. However, rounded, smooth aggregates flow more easily over the aggregates and may improve fresh concrete workability [21].

Contaminants negatively affect the hardened properties of concrete. In a virgin aggregate blend such contaminants are extraneous clays and organic material, however RCA sources typically contain contaminants relating to the demolition site they are obtained from. Most contaminants are found via a visible check at stockpiles and during mixing. Limiting the number of contaminants increases the strength of the concrete. Currently the NJDOT limits the contaminant presence to 10% in RCA [22]. Standard aggregate processing procedures outlined by ACI Committee 221 allow for the control of aggregate parameters which include cleanliness and fine particle removal [23]. RCA production processes follow this standard procedure closely and thus undergo the same treatment [1]. The contaminants in virgin or recycled aggregates are primarily controlled through the quality control/quality assurance procedures at the quarries during crushing procedures.

Sulfate testing measures the capacity of aggregate to withstand intense weathering that occurs during freeze-thaw action. This test is conducted by placing the aggregate in magnesium sulfate or sodium sulfate for an extended time in accordance with ASTM C88-13. These mixtures simulate the formation of ice crystals that can form on aggregates during winter. The Washington DOT found that both virgin and recycled aggregate pass the magnesium sulfate component of the test however only virgin aggregates are able to endure sodium sulfate testing based upon acceptable mass losses.

Due to the contradiction of the results from the two tests, agencies commonly waive RCA soundness testing [20].

Fresh RCA Concrete Properties. The workability of concrete typically refers to how easily it can be set into place and finished. Workability depends on the consistency of concrete mixtures and is commonly indicated through a procedure known as slump testing as specified by ASTM C143 [24]. In laboratory conditions for normal concrete, slump increases proportionally to water content and is inversely related to strength. The acceptable slump value for a concrete mixture is dependent on the structure in which the concrete will be used. These ranges typically fall between 50-100 millimeters for most applications [22]. Recycled aggregates absorb more water due to high porosity, thus concrete made with RCA has been observed to require approximately 5% more water than concrete made with virgin aggregates to achieve the same workability [25]. Pre-saturating RCA prior to mixing can counteract this effect. Brown, et al. concluded that the roundness of RCA produced commercially increased workability when compared with natural basalt aggregate [29]. The pumpability of concrete can be described as its ability to remain well mixed and easily moveable under pressure [27]. This is an important characteristic of concrete because many structures require the use of concrete pumps in order to place material. Pumpability is closely related to workability although it also accounts for the capacity of the mixture to avoid segregation while pumping. Concrete which is not readily pumpable will segregate or create pipe blockages. Ensuring that concrete made with RCA can be used in concrete pumps shares many of the same measures needed to ensure its workability. This includes the pre-soaking of recycled aggregates and strict slump control.

Water expands when freezing by approximately 9% [28]. Concrete that is expected to experience freeze-thaw conditions is required to have air entrainment. Air entrainment produces more distributed air voids in a concrete mixture, allowing water room to expand during freezing [29]. Boyle, et al. determined that the air content of RCA mixes was only marginally greater than concrete made with virgin aggregates, but the values had greater variability [30]. However, the concrete with RCA did show better resistance to cracking during freeze-thaw cycles. The higher air content of the RCA mixture is due to the air voids within the adhered mortar of the recycled aggregate. This study also suggested that target air contents be raised when designing concrete with RCA.

Curing of concrete is a procedure that takes place after mixing and placing concrete in which the moisture and temperature are kept within a specific range for a certain amount of time [29]. Typical curing methods include membrane curing, steam curing and the ponding method [11]. Membrane curing requires covering the wetted material with a waterproof surface for seven days to prevent the evaporation of water. Concrete cured using the steam method requires control of temperature and humidity to prevent the sample from drying out. Concrete cured via this method may achieve 70% of ultimate strength after 28 days. The ponding method entails submerging the concrete surface in water during the curing process. Amorim, et al. found that curing conditions did not tend to affect concrete mixtures with RCA any differently than those with virgin aggregates [31].

Hardened RCA Concrete Properties. In general, the addition of RCA decreased the strength of concrete, though little difference in strength can be found for replacement rates below 30%. As the percentage of RCA goes up, the compressive strength of the

specimen goes down [12, 13, 32, 33]. At 50% and 100% replacement, the compressive strength decreases by 16.6% and 26.4% respectively [34]. Hayles, et al. also concluded that concrete mixtures with RCA failed to meet targeted mixture strengths of 25 MPa and 35 MPa [35]. ASTM C39 and AASHTO T22 may be used to test the compressive strength of a cylindrical concrete specimen.

Abdel-Hay observed the impact of curing conditions in RCA concrete strength gain [36]. Through experimentation, it was found that water curing lead to increased 28-day compressive strength at 25% and 100% RCA replacement, however air curing lead to higher strengths at all ages at 50% RCA replacement. This indicates no obvious link between curing condition and concrete strength at given RCA replacement rates. A replacement rate of 50% is suggested to achieve maximum compressive strength for a concrete mixture with RCA. The compressive strength of RCA mixtures may vary with the RCA used. Corinaldesi found that compressive strength was 8% lower when fine RCA was used rather than a strictly coarse blend of RCA using the same water to cement ratio [37]. Corinaldesi attributed this strength difference to the variation of absorption, porosity, and average dimension of the RCA particles. Davis, et al. found that ASTM #57 coarse aggregates made RCA 10-15% weaker compared to RCA with smaller ASTM #8 coarse aggregates [34].

Concrete does not have a linear stress-strain relationship and so chord modulus is appropriate for determining this relationship as per ASTM C469 [21, 38]. When recycled concrete aggregate is added in to supplement virgin aggregate, the chord modulus of the concrete sample decreases. This decrease can vary widely due to the type and amount of RCA used. On average the decrease in elastic modulus is 15%. Equal or higher elastic moduli have been found when using RCA by the inclusion of additives [39-41]. A more dramatic difference in elastic modulus can be seen with replacement by more than 50% RCA [42].

Porosity is a measurement of the amount of interconnected pores and air voids in a sample of concrete at the interfacial transition zone. This measurement is used to suggest the relative durability of a mixture against freeze-thaw and abrasion [43]. Residual mortar present in recycled aggregates increases the porosity of RCA above virgin aggregate or gypsum. This high porosity allows for sorption into the concrete and the penetration of chemicals. Water absorption in the aggregate is increased which may be detrimental to the concrete's durability [21]. Large or connected voids in concrete may decrease strength and increase permeability [29]. ASTM C642-13 presents standard practice for determining voids in hardened concrete [44]. Additionally, ASTM D4404-10 gives a method of porosity determination in aggregates using mercury intrusion porosimetry (MIP) [45]. As this test is conducted by mercury intrusion under high pressure, it provides accurate analysis considering even very small pore spaces.

Larger pores in RCA create passageways for chemical seepage into the material. When chemicals such as chloride infiltrate a section of reinforced concrete, the steel corrodes and the structure weakens [21]. A high permeability suggests a low strength

value and high porosity of the concrete [29]. RCA can be up to 6 times more permeable than virgin aggregate [1, 46]. Additionally, reducing the water to cement ratio by 5% to 10% may counteract the permeability issues of RCA. Abdel-Hay found that sample permeability is reduced by curing the RCA concrete in water. 100 mm cube samples that were cured in water had sorptivity values that were 50% less compared to those obtained by curing in air at 28-days [36]. Thomas, et al. showed that the high porosity of RCA may lead to higher water and oxygen permeability in concretes using recycled aggregates when compared to those without [47]. This leads to concerns in regard to the durability of RCA especially in instances where aggressive deleterious processes occur such as freeze-thaw action. However, Andal concluded that recycling concrete for aggregate while selecting material for original-mixture-quality preservation characteristics drastically reduced these concerns [48]. However, this process excludes recycled materials that do not reflect the characteristics of the original mixture and thus reduces the amount of material that may be recycled on a job site.

Newly made concrete goes through a phase of drying shrinkage. Due to evaporation and chemical shrinkage, new concrete decreases in volume. After this initial shrinkage, the sample may continue to shrink as it settles which causes cracking in the sample. Meinhold, et al. concluded that drying shrinkage causes an increase in tensile stress and increases linearly as RCA replacement rates increase [39]. Due to RCA's higher absorption, it causes 40-60% more shrinkage than virgin aggregate. Over the course of the first year, the concrete is expected to shrink 65% to 85% more. When RCA was used in mixtures containing fly ash, the drying shrinkage was reduced. Xiao, et al. showed that replacement rates of 50% and 100% RCA resulted in 17% and 59% higher

shrinkage respectively over natural aggregate mixtures [49]. Yamato, et al. found that the use of shrinkage reducer can counteract the effects of RCA [50]. Drying shrinkage can be determined via ASTM C596-09 [51].

Freeze Thaw is the tendency for internal cracking due to the creation of forces inside the concrete when water enters a sample, freezes, and expands. Freeze-thaw durability performance may be assessed using ASTM C666 [52]. While most studies agree that RCA replacement may not notably impact concrete strength, the increased permeability of these mixtures allows freeze-thaw processes to deteriorate the concrete more quickly. Thus the main concern with recycled aggregates is their impact on concrete durability. A study by Yamasaki and Tatematsu confirmed this, showing a marked decrease in freeze-thaw performance for samples with RCA replacement [53]. The negative effects of recycled aggregates in recycled aggregate concrete (RAC) mixtures can be limited effectively by mixture design and the use of additional additives. Yamato, et al. suggested that this reduction in durability can be counteracted in part by limiting RCA replacement, reducing water to cement ratio, and increasing entrained air in the mixture [50]. Salem, et al. confirmed these findings and claimed that entrained air may neutralize the durability differences between virgin aggregate mixtures and RCA mixtures [54]. Additionally, Wei suggested that the addition of calcined diatomite in small amounts (2%) can reduce the permeability of RAC mixtures and improve durability characteristics [55].

Huda and Alam found that increasing RCA replacement rates from 30% to 50% correlated with decreasing relative dynamic modulus throughout the testing [56]. However, it was found that all samples greatly exceeded the passing criteria set forth by

ASTM C666 of 60% of initial elastic modulus at 300 cycles. This study concluded that the use of RCA does not have a significant detrimental impact to the durability of concrete in freeze-thaw conditions. Amorim Jr., et al. found similar results in the testing of concrete with 15% to 50% replacement rates, with instances of concrete with RCA replacement even surpassing the durability factor of samples containing only virgin aggregates [57].

In concrete subjected to sufficient moisture, it is possible for the alkaline cement paste to react with silica found in aggregates in a manner that causes swelling in the concrete [58]. This causes cracking over time in the material. Concrete swelling due to alkali-silica reaction (ASR) can be measured following standard practice ASTM C 1293 [59]. Li and Gress found that this reaction requires a pH threshold to be met within the mixture [60]. The substitution of fly ash into the mixture at a rate of 25% effectively controlled this reaction. It was found that RCA mixtures with a fly ash replacement rate of 25% met all ASTM limitations for ASR swelling. This is due to the pozzolanic reaction depleting calcium in the mixture, which halts the alkali-silica reaction. A study by Thomas, et al. agrees that supplementary cementitious materials such as fly ash, slag, or silica fume at threshold replacement levels effectively limited the alkali-silica reaction in concrete [61]. The study also suggested the use of portland cement with low alkali content as a method of controlling this reaction in low- to moderate-risk scenarios, but suggested a combination of this and SCM incorporation for high-risk cases.

Regulations. The United States Army Corps of Engineers puts forth the United Facilities Criteria (UFC) that applies to the use of recycled concrete aggregates in individual circumstances. These may include pavement surfaces, structures, airfields, heavy-duty pavements, and aggregate base courses. Detailed requirements for usage are as follows.

Concerning concrete pavements, UFC 3-250-04 states that recycled concrete may be crushed and used as both coarse and fine aggregate [62]. This assumed the concrete is crushed to a proper gradation following standard ASTM C33 guidelines. The UFC requires recycled aggregates to be washed only if they are contaminated with base or subgrade material. If the aggregate comes from D-cracked pavement, it must be crushed to 20 millimeters maximum size. Implementing a maximum size prevents D-cracking from occurring again. Aggregate interlock load transfer capacity is reduced but short panel lengths address this issue [63].

UFC 3-250-07 details the procedure for production and use of crushed concrete aggregate [63]. It may be collected from both pavements and structures given that asphalt, subbase, and subgrade materials are removed as thoroughly as possible and all steel reinforcement is removed. Once recycled aggregates are crushed, stockpiled, and have met all requirements for normal aggregates for the intended purpose, they may be treated as such and are usable as unbound or bound cement treated bases, and as per UFC 3-250-04 Standard Practice for Concrete Pavements.

UFGS-32 13 13.06 provides additional information on the use of recycled aggregates in pavements and site facilities [64]. Concrete is allowed as an appropriate recycled material in the use of aggregates for these purposes under the condition that it

complies with ASTM D6155 Standard Specification for Nontraditional Coarse Aggregates for Bituminous Paving Mixtures and gradation following ASTM C33/C33M. This document addresses these standards for coarse aggregate only. Aggregate for use in airfield pavement and other heavy-duty pavements requires a thorough survey of materials, including source, test results, mill certificate data, composition, and service records [65]. These requirements preclude the use of recycled aggregate for these applications.

UFGS-32 11 23 allows the use of crushed concrete aggregates in the base course for road use [66]. Recycled materials must meet ASTM gradation requirements for coarse aggregate. For use in airfield pavement coarse bases, additional alkali-silica reaction testing must be completed before use in accordance with IPRF-01-G-002-03-5, which outlines evaluation techniques for recycled materials to be used in airfield pavement base. For both road and airfield uses, subgrade soil must contain 0.3% or lower sulfates in order to avoid ettringite reactions with recycled aggregates. This is an expansive reaction that causes cracking and swelling. Additionally, risk assessment must be completed for airfield projects in accordance with Engineering Technical Letter 07-6 Risk Assessment Procedure for Recycling Portland Cement Concrete Suffering from Alkali-Silica Reaction in Airfield Pavement Structures [67]. This is done to avoid concrete failures such as cracking as well as damage to adjacent facilities. UFGS-32 11 36.13 also allows the use of recycled aggregates in lean concrete (low cement content) base courses provided it meets the ASTM standards and strength requirement for the intended use [68].

Ternary Blended Cement-Based Binder

The process of making portland cement requires an immense amount of energy and is known to release carbon dioxide into the environment. The inclusion of supplementary cementitious materials (SCM) into portland cement concrete mixtures allows for a reduction in the amount of portland cement needed in the concrete binder, while incorporating other benefits such as increased strength. Consequently, there is much interest in researching and standardizing the addition of SCM into cement concrete [69]. SCM are materials that have cementitious properties on their own, or when combined with portland cement. Therefore, including them into concrete mixtures properly improves fresh mixture properties and hardened concrete properties [68].

Isothermal calorimetry measures the change in heat of a substance undergoing a chemical reaction at a constant ambient temperature. This can be used to measure and identify patterns in the heat of hydration of cement mixtures containing different supplements. This correlates directly with the ultimate strength and durability of the concrete [70]. In general, the hydration of cement occurs in five distinct stages. Upon first contact with water, a rapid heating process begins with a duration of 15 to 30 minutes as a result of ions dissolving in the water and reacting with components of the cement (Stage 1) [71]. This period provides no strengthening characteristics to the concrete; however it can reduce the reaction rate in latter stages [70]. The second part of hydration is a period of dormancy during which hydration stops temporarily (Stage 2). During this time, the concrete does not generate heat and is in a workable condition. This stage may last upward of 5 hours and can be retarded by the inclusion of supplementary materials and additives. Following the dormant phase, hydration of tricalcium silicate

(C_3S) and dicalcium silicate (C_2S) accelerates in a concrete-strengthening reaction that produces a significant amount of heat (Stage 3). Following this accelerated hydration stage, hydrate layers thicken and there is less available surface area of unhydrated particles, slowing the hydration reaction (Stage 4). During this portion of the reaction, C_3A hydration may occur and will cause a secondary peak in heat of hydration. The magnitude of this secondary reaction is dependent on the inclusion of pozzolanic materials in the mixture and will increase significantly with their addition. Finally, the reaction reaches a steady state where little or no hydration occurs (Stage 5). The figure below shows the general heat of hydration curve for portland cement concrete as provided by Kosmatka, et al. [18].

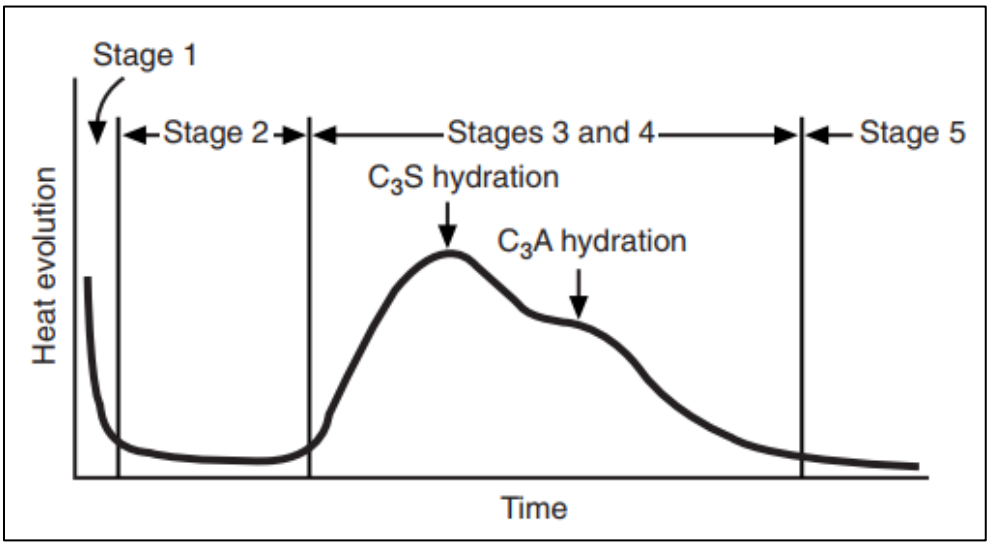

Figure 1. Hydration curve for portland cement concrete [18].

Total heat of hydration is an indicator of completion of reaction in a mixture and thus the analysis of these reactions through calorimetry is effective in explaining the strength and durability of individual ternary mixtures.

When selecting components and proportions for a concrete mixture, there are several factors to be considered. Dewar suggested considering the following parameters: consistency, stiffening rate, cohesion, density, strength, durability, and air content [72]. Requirements in these categories impact the chosen mixture and the method of proportioning. Concerning individual tests, there are additional factors that must be considered in a real-world scenario. Materials should accurately represent those to be used in construction and should be in similar condition to avoid discrepancies between results in laboratory and field evaluations. Smaller test batches will lose water content more easily to evaporation and absorption. Lastly, multiple initial tests are preferred when used as a representation of larger-scale mixtures.

Dewar has cataloged several mixture design methods. The British Ready Mixed Concrete Association (BRMCA) proposes mixture design based on the plastic properties of the concrete and measurement of hardened performance [72]. Dewar proposed an addition to this process based on a computer model of gradation, bulk density and relative density of aggregates. The goal is to model the interaction between particles accurately as to avoid the need for preliminary trial mixing. The American Concrete Institute suggests ACI 211.1-91 as a guideline for selecting proportions for cement concrete made with other cementitious materials [73]. This document outlines the procedure for determining mixture proportions by weight equivalency and conversion of absolute volumes to weights, dependent on specifications regarding water-to-cement ratio, cement content, air content, required slump, aggregate size, and strength. Kansas Department of Transportation (KDOT) provides a solution for absolute volume design dependent on the known required volumes of each component of the mixture [74].

Hydraulic cements are materials that demonstrate cementitious properties when mixed with water, such as portland cement. Excluding portland cement, these are considered secondary cementitious materials. Blended hydraulic cements are those that include portland cement along with other hydraulic SCM. These types of SCM include materials such as slag cement and Class C fly ash. Slag cement is a byproduct of the operation of iron blast furnaces, and it has been found to increase set time and concrete strength [75]. Fly ash is a byproduct of coal burning and is usually separated into two classes for use in cement. Class C fly ash is described as sometimes exhibiting cementitious properties and contains more calcium oxide [36]. Its effects on concrete can include needing less water to achieve a set workability, increased strength, and reduced heat of hydration.

Another type of SCM is pozzolans. These are not cementitious on their own, but are when combined with calcium hydroxide, a chemical found in hydrating cementitious materials. There are various types of pozzolans that are added to portland cement concrete. These can include Class F fly ash, silica fume, and other natural pozzolans. Class F fly ash is described as being only pozzolanic and containing less calcium oxide than Class C. Silica fume is a byproduct of making silicon and ferrosilicon alloys. Pozzolans can strengthen concrete by furthering the production of calcium silica hydrate (CSH), a strengthening reaction product in hydraulic cements. The addition of silica fume may increase strength of the cement though the mixture requires a higher water to cement ratio [76]. Using these products is advantageous in that cement production is a primary producer of carbon dioxide and using replacement pozzolans helps lower greenhouse gas emissions. Natural pozzolans were originally used as SCM and include materials such as

volcanic ash, calcined clay, calcined shale, and metakaolin [36]. One of the greater points of interest concerning SCM is decreasing the amount of variability between producers as most SCM are byproducts and their actual compositions can differ depending on when they were produced. Decreased variability in the materials can lead to more accurate, consistent testing results.

Limestone is another material that may be used to lessen the environmental impact of concrete. Blending limestone and portland cement is a fairly new practice. In 2012 ASTM defined portland limestone cement (PLC) as containing 5% to 15% limestone [77]. PLC is made by adding limestone to the cement clinker before it is ground. The limestone is softer than the clinker so it may be crushed into finer particles than cement, creating a greater particle size distribution in the binder. The purpose of PLC is to improve the environmental performance of cement. Limestone may affect the set time, compressive strength, and permeability of concrete [78]. Finer limestone may decrease the setting time and these fine particles increase density and lower permeability. Low concentrations of limestone increase early strength. However, when the cement is more than 15% limestone it may negatively impact compressive strength. When paired with Class C Fly Ash and slag, the compressive strength of concrete increases [78].

Fresh Ternary Blended Concrete Properties. The inclusion of SCM may affect the required setting time of a concrete mixture. Setting time affects the construction logistics as the concrete needs to be transported and placed before setting occurs. After it is placed, it then needs to be consolidated or formed. Ghosh, et al. found that when Class C fly ash is used to replace 20% of Type I portland cement, initial and final setting time can be increased by 96 and 189 minutes, respectively [69]. Class C may be more

effective than Class F at increasing setting time when it has a higher content of oxides or sulfur. Larger increases in setting time occurred when Class C fly ash was mixed into a ternary mixture with Class F. Time to set was increased by 402 minutes compared to a control mixture of portland cement only [69].

Hardened Ternary Blended Concrete Properties. Bektas, et al. investigated the trends that binary and ternary blended concretes exhibited in their hardened properties [79]. The study found that in binary mixtures of additives and portland cement, adding Class C fly ash provides similar compressive strengths at 15% and 30% to that of control samples of portland cement. Ternary blends of Class C fly ash and slag showed improved strengths. The inclusion of Class F fly ash lowered compressive strengths at 28 days independent of replacement rate, however the inclusion of slag and Class F fly ash produced greater strengths. Hariharan, et al. analyzed the effects of ternary blended binders of fly ash and silica fume on compressive strength and chloride ion permeability [80]. It was observed that the use of silica fume increased the early and final strength of concrete compared to a control. When Class C fly ash was mixed with the silica fume, the silica fume was also found to have a positive effect on the compressive strength of the concrete and accelerated the early strength. An optimal compressive strength was found using 30% Class C fly ash and 6% silica fume. The study also found that, except for the mixture designed for maximum strength, the difference in compressive strength between the control mixture and the binary and ternary blended concrete mixtures was negligible [80].

Air void systems are a required part of concrete and have a large effect on the mechanical properties of a mixture. Air void systems consider the air content, spacing factor, and specific surface of voids in fresh and hardened concrete. Having a well formed air void system may increase the durability of concrete under freeze-thaw conditions. Bektas, et al. provides that a good air void system has a spacing factor of less than 0.2 mm in hardened concrete [79]. The addition of SCM does not have obvious trends on air void systems. High dosages of silica fume may have a negative effect on air voids [79, 81].

When cement is mixed, a byproduct of the chemical reaction is the release of heat. In general, ternary blended concrete have a lower heat of hydration than portland cement alone [82]. Portland cement with slag takes longer to set and as such releases heat over a longer period of time than portland cement alone. This leads to a lower peak temperature of mixtures with slag [81]. When the percentage of fly ash is increased and the percentage of slag is decreased, the overall heat signature decreases.

Due to sourcing and mixing procedures, drying shrinkage in ternary blended cement concretes is difficult to examine as the additives have inconsistent effects on the hardened property [81]. The addition of high doses of silica fume or slag increases drying shrinkage. Volume stabilization is seen in ternary blends of portland cement, silica fume, and slag or fly ash. Shrinkage is generally reduced with a reduction of SCM usage. At higher percent replacements such as 30% slag and 20% fly ash with portland cement, the mixture may be unable to resist drying shrinkage and are more susceptible to cracking [82].

Freeze-thaw durability is a measure of the capacity of a hardened concrete mixture to resist cyclic degradation processes. In areas of harsh or varied weather conditions, freeze-thaw testing may gauge the effect that the environment will have on the finished concrete. Stundebeck offered that air void structure and air entrapment of a sample has a great effect on its freeze-thaw resistance [83]. The use of silica fume creates a refined pore structure which may aid durability, though more than 5% silica fume was not found to increase resistance any further [81, 83]. Stundebeck also found that replacing portland cement with slag gives a greater risk of surface damage and freeze-thaw damage than replacement by fly ash. Mixtures with silica fume, portland cement, and fly ash also have lower freeze-thaw resistance.

Blended Cement Mixtures with RCA (B-RCA)

Blended, recycled aggregate concretes (B-RCA) achieve the environmental, economic and materials properties benefits of both binder admixtures and aggregate substitution when properly used. However, mixtures including RCA and SCM also incur the negative impacts on the mixture associated with both. This can include the chemical and physical aggregate properties as well as binder properties and interactions.

Fresh B-RCA Properties. Mixtures incorporating RCA require more water in order to maintain a comparable workability to virgin aggregate concrete mixtures. Guardián, et al. found that concrete slump decreases when RCA levels increase, however when 35% fly ash is added, the slump begins to stabilize and equal the control blend [84]. Kim, et al. finds that adding 30% of fly ash increases the slump of RCA mixtures by a 45% to 100% [85]. The density of concrete mixes only slightly changes when low levels of fly ash and/or RCA are introduced. The following table shows how density changes

based upon the concrete blend, presented by Blezynski, et al. and gathered by Sadati, et al., Cong, Pepe, Kou and Poon, and Lima, et al. [86-90].

Table 1

Density of Concrete with Recycled Concrete Aggregates

Concrete Mixtures	Density (kg/m^3)
Conventional Materials	2211-2365
Fly Ash and Coarse RCA	1958-2324
Fly Ash and Fine RCA	1958-2299

The fresh density of concrete mixes decreased when RCA and FA increased. Mixes with a higher water-cement ratio were less affected than those with low w-c ratios when RCA and FA were introduced.

Hardened B-RCA Properties. The presence of adhered mortar on recycled aggregates impacts the ability of fresh mortar to adhere to RCA and may impact mixture strength. Akbari and Rushabh found that the compressive strength of recycled aggregate concrete with ternary blended binder is typically at least 76% of that of a virgin mix [91]. The strength of the original pavement which is recycled along with the strength of the new mix contribute to the strength of a mixture of concrete containing RCA. The percentage of RCA used and the aggregate size proportion also contribute to the strength of the mixture. The study found that compressive strength increased with increasing RCA replacement, with a maximum strength identified between 30% and 40% recycled aggregate replacement. When introducing secondary cementitious material (SCM) such as fly ash and silica fume, the adherence was improved between the recycled aggregate

and the paste. The optimum percentage of SCM was found to be 5% silica fume and 20% fly ash without recycled aggregate and 20% fly ash, 10% silica fume with recycled aggregate at a replacement rate of 50% [91].

Chapter 3

Materials Identification

Table 2 provides the raw materials used in testing as well as suppliers from which the materials were procured.

Table 2

Project Materials

Material	Source
Portland Cement, Type I	Keystone Cement Co.
Silica Fume	BASF Co.
Ground, Granulated Blast Furnace Slag (GGBFS), Grade 100	Lehigh Hanson, Inc.
Fly Ash, Class C (FAC)	Headwaters, Inc.
Fly Ash, Class F (FAF)	Salomone Bros., Inc.
Recycled Concrete Aggregate (#57)	Salomone Bros., Inc.
Virgin Coarse Aggregate (#57), Trap Rock	F. J. Fazzio, Inc.
Fine Aggregate (F.M. = 2.65)	F. J. Fazzio, Inc.
Air Entraining Admixture	Sika Corp.
Water Reducing Admixture	Sika Corp.

Portland cement and four supplementary mineral admixtures were addressed in this study. These were ground, granulated blast furnace slag, Class C fly ash, Class F fly ash and silica fume. X-ray fluorescence (XRF) was used to determine the oxide composition of each mineral as given in Table 3. Figure 2 provides the gradations for the three aggregates used in experimentation. Table 4 provides additional characteristics for each aggregate.

Table 3

Cementitious Material Oxide Composition

Component	Portland Cement	Fly Ash Class C (FAC)	Fly Ash Class F (FAF)	GGBFS	Silica Fume
SiO_2 (%)	19.32	28.13	39.01	25.69	94.23
Al_2O_3 (%)	5.77	13.49	22.75	10.35	0.37
Fe_2O_3 (%)	2.38	8.97	24.79	0.51	0.32
CaO (%)	61.55	37.30	5.97	56.33	2.23
MgO (%)	2.63	2.87	0.63	3.54	0.27
SO_3 (%)	4.56	3.02	1.47	1.76	0.30
Na_2O (%)	0.33	1.00	0.37	0.13	
K_2O (%)	0.97	0.85	2.98	0.45	1.55
TiO_2 (%)		2.08	1.43	0.77	
P_2O_5 (%)		1.28	0.35	0.02	0.16
ZnO (%)			0.03		0.26
MnO (%)				0.22	0.09
Others (%)	2.49	1.01	0.22	0.24	0.13

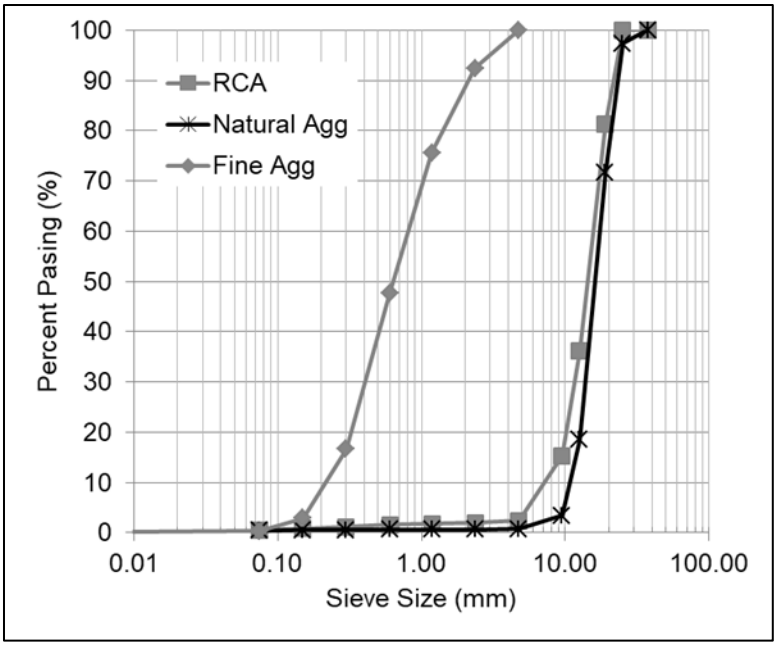

Figure 2. Aggregate gradations.

Table 4

Aggregate Properties

Sample Type	Bulk Specific Gravity DRY	Bulk Specific Gravity SSD	Absorption, %
RCA	2.38	2.49	4.71
Virgin Aggregate	2.76	2.77	0.20
Fine Aggregate	2.60	2.62	1.04

Chapter 4

Methodology

Experimentation was segmented into two tasks. Task 1 was blend optimization, which included all procedures for optimizing the ternary binder composition which was used for full-scale RCA concrete mixtures. First, mortar cubes were mixed for all binder combinations of portland cement and mineral admixtures proposed in this research. Second, isothermal calorimetry was conducted for each mixture in order to observe curing characteristics and identify interactions between additives. Third, a statistical analysis was performed on mortar cube strength data to find an optimized solution for the binder proportions which produce the highest predicted strength for each blend of mineral admixtures. Finally, fresh mixture tests, surface resistivity, alkali-silica reaction and concrete compression tests were conducted for each optimized ternary blend to compare strength gain and resistivity characteristics for each blend. From this data a single blend was chosen for further testing in RCA concrete. The second task was the testing of ternary blended concrete with RCA replacement. Additional large-volume concrete batches were mixed to compare fresh and hardened properties between a control and ternary blended concrete with varying levels of RCA replacement.

Blend Optimization

Mortar Compressive Strength. Tests were conducted to evaluate the performance of 25 unique blends of cementitious materials. Mixture proportions, listed in Table 5, were determined by percentage mass of total cementitious material to create a design matrix. The notation includes each mineral component followed by that component's percentage by mass. Maximum replacements of 30%, 25%, 25%, and 5% were used for slag, Class C, and Class F fly ashes and silica fume, respectively. These

limits were established based upon New Jersey Department of Transportation recommended practice and a previous study conducted by Taylor, who suggests a maximum portland cement replacement rate of 60% [92]. Rupnow also observed improved physical properties for some combinations of ternary blended cements at 50% portland cement replacement and recommends a maximum portland cement replacement rate of 70% [93]. Intermediate replacement rates were chosen at equal intervals between minimum (0%) and maximum replacement rates. Thus, one mix was portland cement, four were binary blended cements, and the remainders were ternary mixes.

50 millimeter mortar cubes were mixed following ASTM C305. The mortar water-to-binder ratio (w/b) was 0.45, and the ratio of the binder to fine aggregate by mass was 0.50. Triplicates were produced for each mix to be tested for compressive strength at 28 and 56 days. Batches were mixed and molded following ASTM C109. Cube specimens in molds were stored in a moist closet for 24 hours, at which point, cubes were de-molded and placed in a lime-saturated water curing bath. Prior to testing, cubes were removed from the bath, surface-dried, and cleared of any debris. The compression testing configuration conforms to ASTM C109, at a loading rate of 1350 ± 450 Newtons per second. Peak load at sample failure was recorded for each test.

Table 5

Tested Mixture Matrix

Mixture	PC (%)	FAC (%)	FAF (%)	SF (%)	GGBFS (%)
PC100	100	0	0	0	0
PC75FAC25	75	25	0	0	0
PC75FAF25	75	0	25	0	0
PC95SF5	95	0	0	5	0
PC70GGBFS30	70	0	0	0	30
PC45FAC25GGBFS30	45	25	0	0	30
PC55FAC25GGBFS20	55	25	0	0	20
PC65FAC25GGBFS10	65	25	0	0	10
PC57.5FAC12.5GGBFS30	57.7	12.5	0	0	30
PC67.5FAC12.5GGBFS20	67.5	12.5	0	0	20
PC77.5FAC12.5GGBFS10	77.5	12.5	0	0	10
PC70FAC25SF5	70	25	0	5	0
PC72.5FAC25SF2.5	72.5	25	0	2.5	0
PC82.5FAC12.5SF5	82.5	12.5	0	5	0
PC85FAC12.5SF2.5	85	12.5	0	2.5	0
PC45FAF25GGBFS30	45	0	25	0	30
PC55FAF25GGBFS20	55	0	25	0	20
PC65FAF25GGBFS10	65	0	25	0	10
PC57.5FAF12.5GGBFS30	57.7	0	12.5	0	30
PC67.5FAF12.5GGBFS20	67.5	0	12.5	0	20
PC77.5FAF12.5GGBFS10	77.5	0	12.5	0	10
PC70FAF25SF5	70	0	25	5	0
PC72.5FAF25SF2.5	72.5	0	25	2.5	0
PC82.5FAF12.5SF5	82.5	0	12.5	5	0
PC85FAF12.5SF2.5	85	0	12.5	2.5	0

Isothermal Calorimetry. Isothermal calorimetry was used to measure the energy release of paste samples during the hydration process. This was used to measure and identify patterns in the heat of hydration of cement mixtures containing different supplementary materials. The test results may correlate directly with the gain and

ultimate strength of concrete [94]. Total heat of hydration is an indicator of the extent of the reaction in a mix, and thus the analysis of these reactions through calorimetry is effective in explaining the strength and durability of individual ternary mixes.

A high-precision calorimeter was used to measure the energy released during hydration. The machine was calibrated according to manufacturer specifications for 20˚C using calcium sulfate hemihydrate, a manufacturer-supplied reference material. The testing of the cementitious pastes was conducted in compliance with ASTM C1679. All test samples consisted of 50 grams of cementitious material proportioned by mass according to Table 5 with a water-to-binder ratio of 0.50. Prior to testing, materials were stored at 20˚C for 24 hours to minimize temperature differential at the beginning of testing. Samples were hand-mixed with a plastic stirrer in manufacturer-provided sample containers over a period of 45 seconds. The date and time were recorded at the beginning of mixing, approximated to the nearest minute. Two tests were conducted simultaneously, and data was collected per minute for 72 hours. The cumulative heat of hydration (Joules) and power (Watts/gram cement) were recorded for each test.

Ternary Blended Concrete with RCA Replacement

Four mixtures were prepared in order to assess the performance of RCA in a ternary blended concrete. A mixture with only portland cement binder and no RCA substitution was prepared as a control. Then, a mixture with 30% coarse aggregate replacement was prepared in order to identify the effects of RCA replacement. Third, a 30% replacement mixture using the ternary blended binder was produced to assess the performance alterations due to the proposed binder blend. Lastly, a mixture was prepared using the ternary-blended binder at 50% coarse aggregate RCA replacement to assess

high replacement strength and durability. For each mix which included recycled aggregate, the RCA portion of the coarse aggregate was pre-soaked 24 hours before mixing to account for the effect of high porosity on fresh mix properties. All mixture proportions are included in the results and discussion. Table 6 provides a schedule of tests which were conducted, mix volume, and applicable testing standards. In all cases, fresh and hardened concrete test procedures follow the addressed ASTM standard. Compressive strength, elastic modulus, and resistivity were tested at 3, 7, 14, 28, 56 and 90 days. Modulus of rupture was tested at 28 and 90 days. Required volume indicates mix volume needed for the appropriate testing procedure. Bolded volumes were summated to attain required batch volume. In all cases, this was 0.15 cubic meters (c.m.).

Fresh properties were tested to ensure mixtures were comparable. In all cases, slump was controlled via the addition of water reducer to maintain a target of 25 to 50 millimeters. Control for workability ensured that the hardened properties of each batch can be compared on the assumption that fresh mixture behavior is similar. Target air void content was 6.0% ± 1.0 to promote proper durability to freeze-thaw cycling. Unit weight and setting time were recorded for logistical purposes.

Table 6

Ternary Blend (TB)-Recycled Concrete Aggregates (RCA) Test Schedule

Property	Required Volume (c.m.)	Test Method
Fresh Concrete Properties		
Slump	0.006	ASTM C143/ AASHTO T 119
Air Content	**0.007**	ASTM C231/ AASHTO T 152
Air Voids System	-	AASHTO T 348
Unit Weight	0.007	ASTM C 138/ AASHTO T 121
Setting Time	**0.007**	ASTM C403/ AASHTO T 197
Hardened Concrete Properties		
Compressive Strength	**0.030**	ASTM C39/ AASHTO T 22
Electrical Resistivity	0.030	ASTM C1760/ AASHTO T 95
Alkali-Silica Reaction	-	ASTM C1260
Modulus of Rupture	**0.078**	ASTM C78/ AASHTO T 97
Elastic Modulus	0.030	ASTM C469
Drying Shrinkage	**0.005**	ASTM C157/ AASHTO T 150
Resistance to Cyclic F-T	**0.009**	ASTM C666/ AASHTO T 161

Chapter 5

Results and Analysis

Binder Optimization

Mortar Cube Strength. Results for the 28-day and 56-day mortar cube average compressive tests are shown in Figure 3. The bars represent (from left) compressive strength of a mortar with a portland cement only binder, then binary binders, while the remaining results are from ternary binders. The ternary binders are grouped by Class C fly ash with slag (FAC-GGBFS), Class C fly ash with silica fume (FAC-SF), Class F fly ash with slag (FAF-GGBFS), and Class F fly ash with silica fume (FAF-SF), all with portland cement. Full tabulated strength data is available in Appendix A.

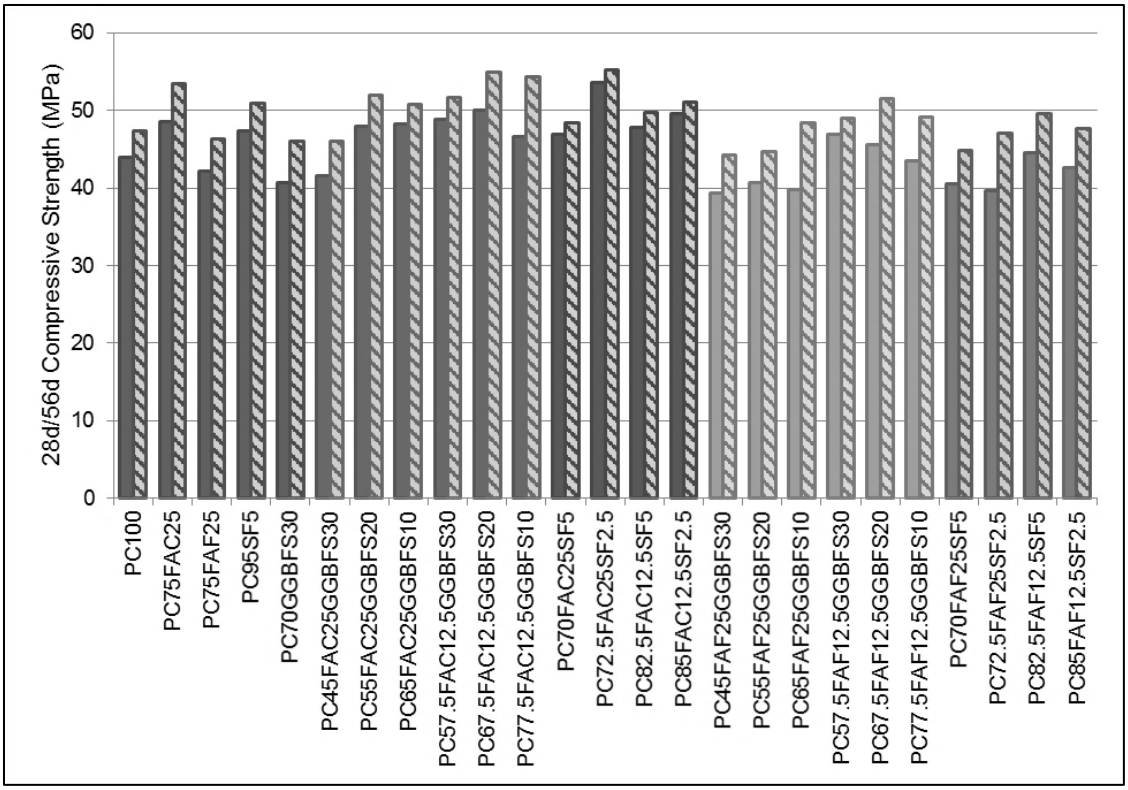

Figure 3. Mortar compressive strength results for 28-day (solid bars) and 56-day (hatched bars) strength for mixtures tested.

Comparing the binary combinations results to the PC results, replacement of PC with Class C fly ash or silica fume are shown to be effective in increasing compressive strength at 28 and 56 days. On the other hand, replacement of PC with Class F fly ash or GGBFS has a slightly lowering effect on compressive strength at 25% and 30% replacement, respectively. Comparing the ternary combination results to the PC results, it is observed that the ternary combinations with Class C fly ash produce higher strengths than PC, except for PC45FAC25GGBSF30 which has the least amount of portland cement in the group. With the Class F and GGBFS combination, the compressive strength becomes lower than the strength of portland cement when Class F fly ash is at 25%, except for PC65FAF25GGBFS10, which has a similar 56 day strength to PC 56 day

strength. For the Class F fly ash and silica fume combination, the compressive strengths are lower or equal in strength to PC strength, except for PC82.5FAF12.5SF5 which has a higher 56 day compressive strength compared to PC compressive strength.

Isothermal Calorimetry. Calorimetry tests were conducted on all binder combinations listed in Table 5. Heat of hydration curves plotted as the thermal power emitted by the binder hydration and reactions over time can be found in Figure 4 to Figure 8. The figures are grouped by blend compositions.

The first group includes Type I cement paste and four binary blended binders, Figure 4. The cement paste heat of hydration curve shows a main peak at 11.5 hours and a sulfate depletion point at 16 hours. The main peak is primarily due to dicalcium silicate (C2S) and tricalcium silicate (C3S) hydration reaction. The peak heat of hydration produced by cement is higher than the peak of the binary blends. The pattern of the heat of hydration with 5% silica fume is similar to the cement curve, only that lower values were produced. The curve for binary blend with 25% Class F fly ash has a main peak that is much lower than the cement paste main peak, but occurs at a similar time. It has a second peak (after the main) at 28 hours, which is due to the secondary tricalcium aluminate (C3A) reaction [95]. However, the heat of hydration curve for the binder with 25% Class C fly ash had its main peak 4 hours after the portland cement paste. Its second peak can also be observed to be higher than its main peak. With the paste containing 30% GGBFS, the main peak is lower that the main peak of the paste with only portland cement, but occurs at a similar time. Its second peak is slightly lower than its main peak, much more pronounced than the Class F fly ash curve and not as high as the Class C fly ash curve. Comparing the presence of GGBFS and Class C fly ash in the binder indicates

that the GGBFS has more hydrating calcium silicates while Class F fly ash had more calcium aluminates reacting during the early age.

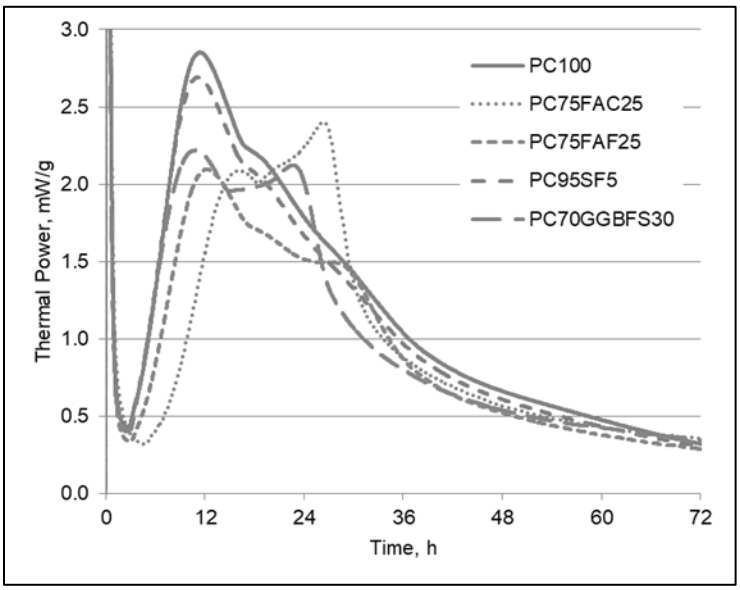

Figure 4. Plot of thermal power vs time of Type I cement and binary binders.

Figure 5 presents results for ternary blends of Class C fly ash and GGBFS. In cases of very high replacement rates, the secondary reactions shown by the second peak overtake the initial C_2S, C_3S reactions by a significant margin. This manifests as a delayed strength gain in the curing process. Low replacement mixes (see PC77.5FAC12.5GGBFS10) maintain a more significant C_2S, C_3S reaction. Figure 6 shows blends of Class F fly ash and GGBFS. These mixes are characterized by a markedly lower peak thermal output with respect to other mixes as a result of high replacement rates with Class F fly ash in addition to significant replacement by pozzolanic materials.

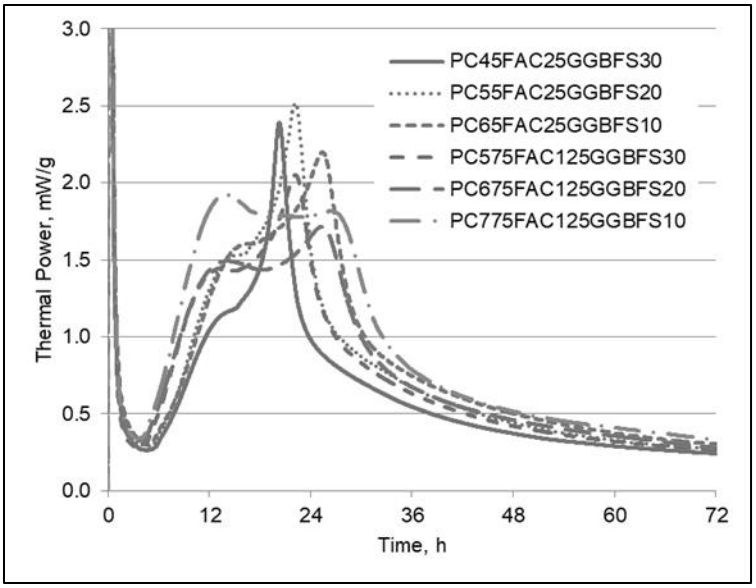

Figure 5. Plot of thermal power vs time of ternary blends of PC-FAC-GGBFS.

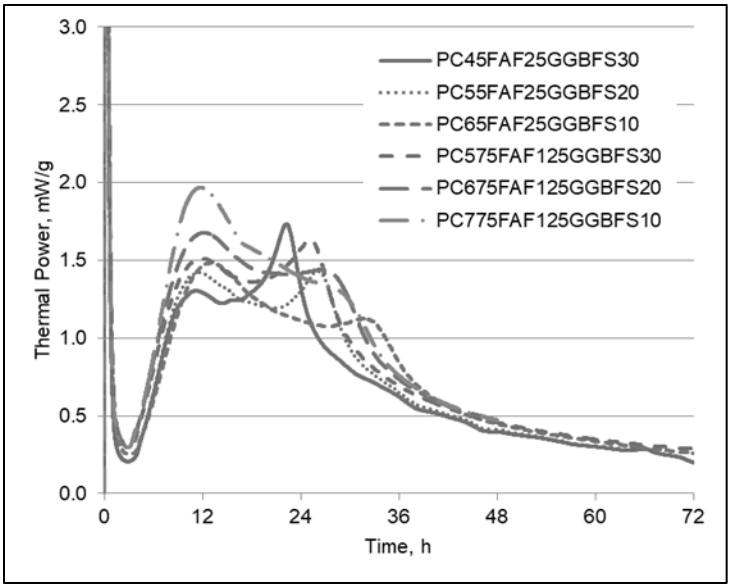

Figure 6. Plot of thermal power vs time of ternary blends of PC-FAF-GGBFS.

Mixes containing Class C fly ash and silica fume are presented in Figure 7. Shown previously, high replacement with Class C fly ash favors the C_3A reaction. There is no apparent interaction with silica fume in this ternary mixture. Figure 8 gives Class F

fly ash and silica fume combinations. These are marked by low thermal peaks and further reduced heat with an increase in either supplementary material.

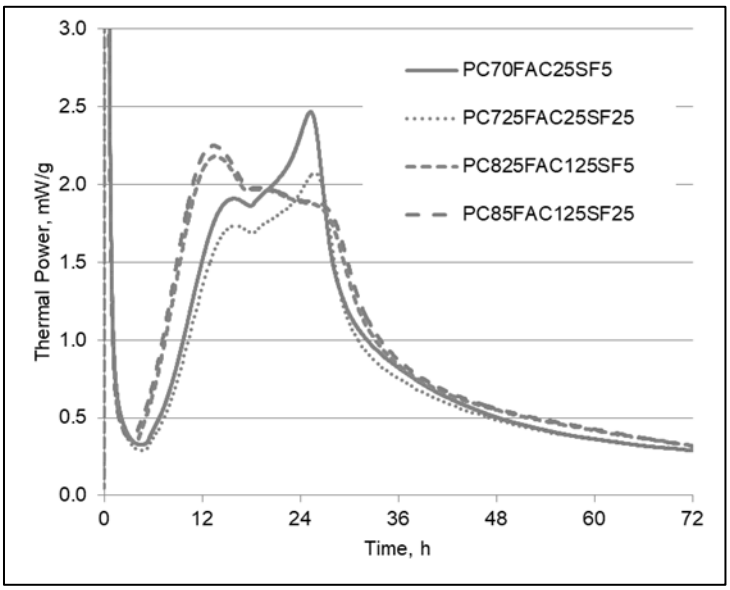

Figure 7. Plot of thermal power vs time of ternary blends of PC-FAC-SF.

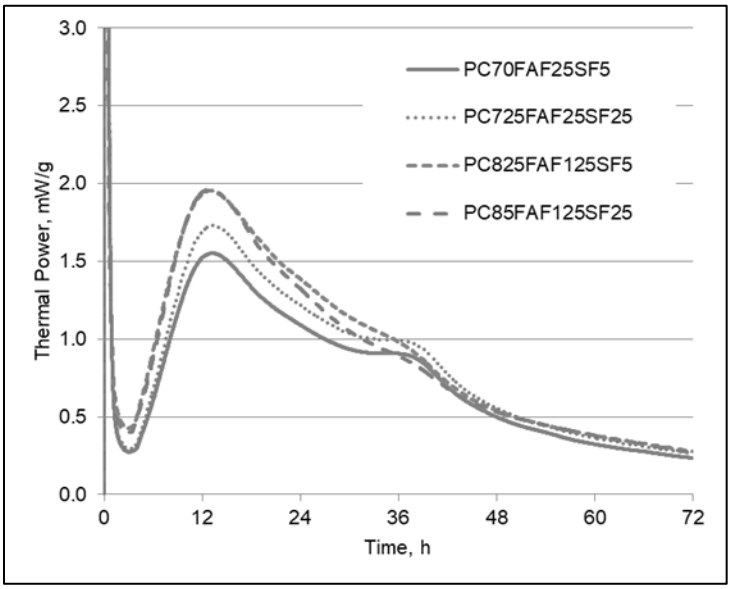

Figure 8. Plot of thermal power vs time of ternary blends of PC-FAF-SF.

The total heat of hydration is determined from thermal power plots by integration of the area under the curve. A comparison of all conducted tests can be seen in Figure 9. There is a consistent trend of reduced heat of hydration with an increase in SCM use for ternary blended cements. However, it was observed that total heat did not necessarily correlate with peak thermal activity. As such, it is not clear that there is a reduced completion of reaction in low-heat blends. From the binary blends, it can be seen that GGBFS has greater reactivity compared to the fly ashes. Even with greater portland cement replacement, the paste with GGBFS released more heat compared to the pastes with fly ash. In the Class C fly ash and GGBFS combinations, the GGBFS complements the fly ash. A higher or equal amount of heat is produced with higher amounts fly ash at about the same level of total portland cement replacement. In the Class F fly ash and GGBFS combination, the heat of hydration indicates little or no interaction between the supplementary cementitious materials; with about the same level of total replacement, a higher proportion of GGBFS will produce a higher amount of heat of hydration. In silica fume and fly ash combinations, Class C fly ash with silica fume tends to have a higher heat of hydration. A lower proportion of silica fume to the amount of Class C fly ash seems to favor reducing the heat of hydration, while a high proportion of silica fume to Class F fly ash seems to increase the heat of hydration.

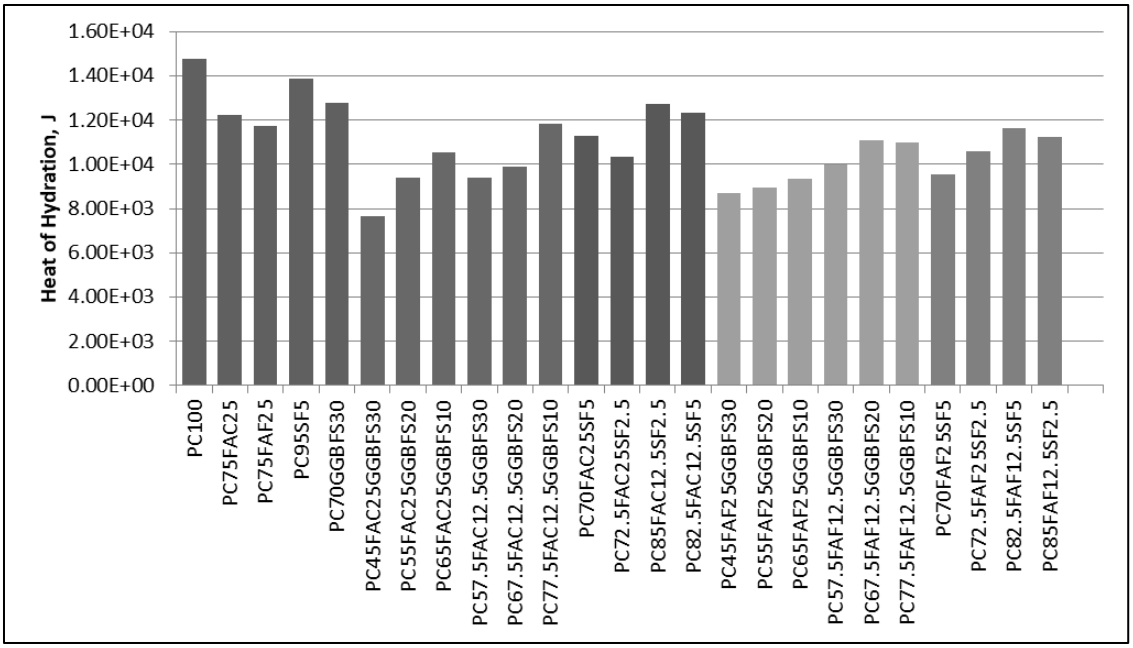

Figure 9. Total heat of hydration for all blends.

Statistical Analysis. The 28-day and 56-day compressive strength test data was analyzed using statistical analysis software JMP. When the 28-day and 56-day strength data was analyzed by percent portland cement used in each mix, it was determined in both datasets that the percentage of the cementitious material that was PC does not impact the average compressive strength above 55% replacement. These plots can be seen in Figure 10. The diamonds in the figures illustrate a sample mean and 95% confidence interval. The line across each diamond represents the group mean and the vertical span represents the 95% confidence interval for each group. As seen in Figure 10, there is no obvious trend in average strength with total cement replacement value, which may suggest that the type of SCM used in each mix and the interactions between the PC and SCM have a more significant effect on the ultimate strength of the concrete than the fraction of PC used within the ranges considered in this study. It can be noted however

that the mean strength of 45% PC is much lower than the mean strengths of 55% PC and greater.

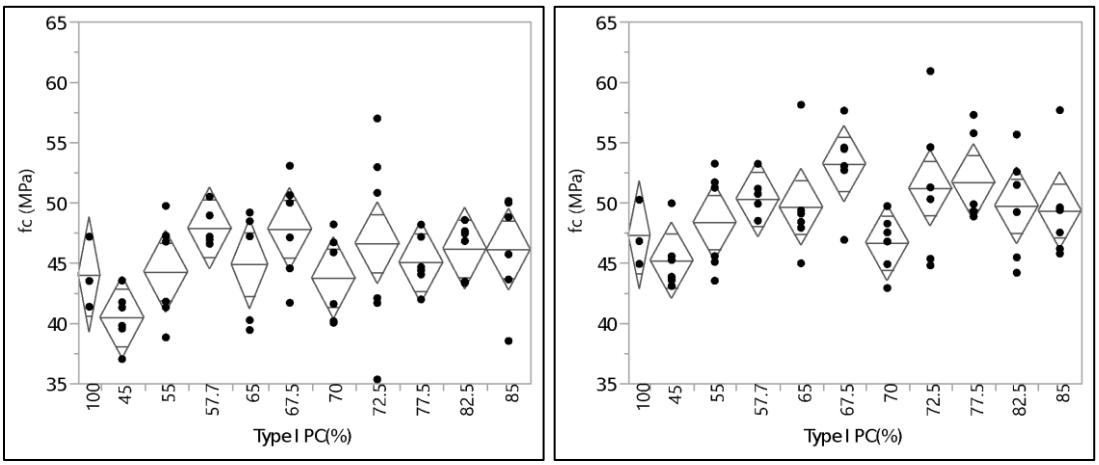

Figure 10. Scatterplot of 28 day (left) and 56 day (right) compression data by % PC.

Surface plots were made to model the relationship between the replacement rates of supplementary cementitious materials and the predicted compressive strength from the data collected in the mortar cube tests. The x- and y- axes each represent the percent replacement of one SCM being analyzed and range from 0% to maximum replacement rate tested along each of these axes. Thus the origin point represents no replacement (Type I portland cement), and data points which lay on an axis represent binary blends with replacement by only a single SCM. There are four such plots created representing the studied combinations of SCM seen in Figures 11 through 14. Optimal mix designs were selected based on the 56-day strength (f'c) analysis as this represents closest the ultimate strength of the mix.

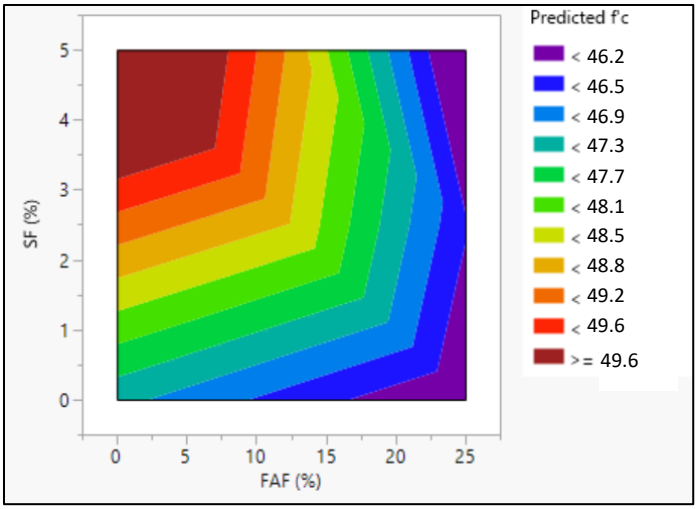

Figure 11. Class F fly ash and silica fume data surface plot.

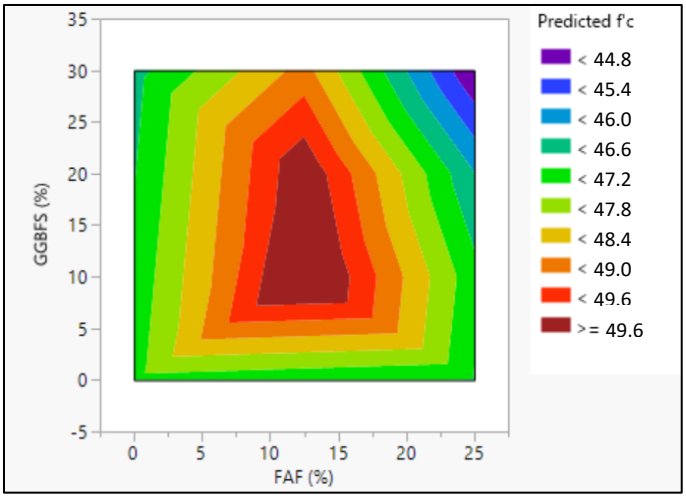

Figure 12. Class F fly ash and slag data surface plot.

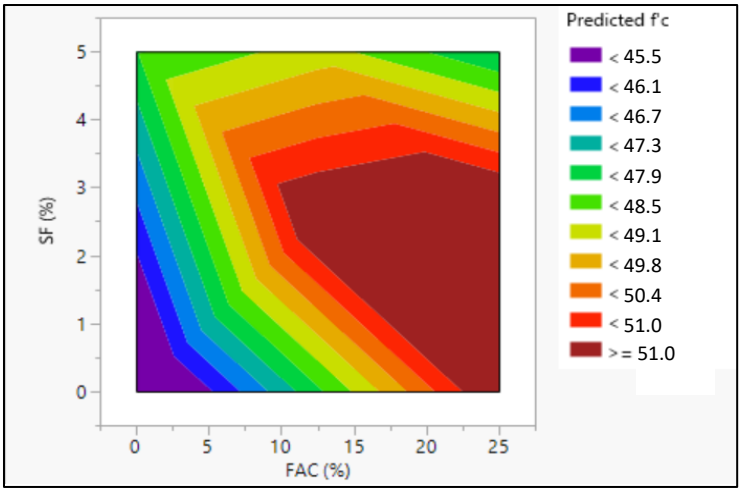

Figure 13. Class C fly ash and silica fume data surface plot.

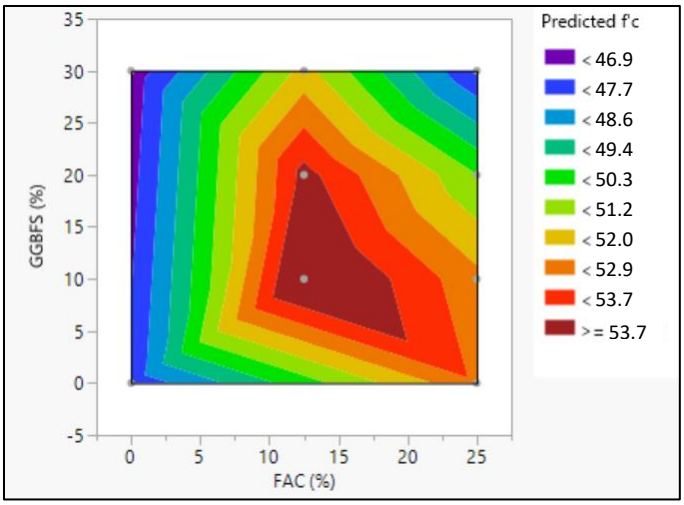

Figure 14. Class C fly ash and slag surface plot.

Based on this analysis, Table 7 was produced. These results include optimal SCM replacement rates for each ternary blend within the studied percent replacement of Type I portland cement ranges found using the surface plots, as well as total replacement rates and predicted mortar compressive strengths for each combination. These predicted compressive strength values were calculated by inputting the optimal percentages of each

material found using the surface plots into the function of the corresponding surface given by the statistical software. It is noted that in the case of PC-FAF-SF combination, an optimum combination excludes FAF, which makes it a binary binder. Among the three SCM combinations in Table 7 that are ternary combinations, FAC-GGBFS has the highest strength and highest total heat of hydration at 72 hours curing within the studied range of percent replacement of type I portland cement. FAC-SF has the lowest total heat of hydration, but is second highest in strength. The predicted 56-day compressive strength of the optimal mixes was compared to the experimentally found compressive strength at 56-days.

Table 7

Optimized Ternary Blends

SCM	PC (%)	FAC (%)	FAF (%)	GGBFS (%)	SF (%)	% SCM by weight	Predicted 56 day Strength, MPa	Tested 56 day Strength, MPa	Total Heat of Hydration (50g), kJ
FAF-SF	95		0		5	5	51.1	47.3	13.86
FAF-BFS	77.5		12.5	10		22.5	50.7	49.1	11.0
FAC-SF	72.5	25			2.5	27.5	52.5	55.3	10.36
FAC-BFS	77.5	12.5		10		22.5	54.9	54.3	11.81

Ternary Blended Concrete. 100 millimeter diameter concrete cylinders were mixed for each of the three ternary binder proportions listed in Table 7. Table 8 gives the mixture proportions used. Proportions for a comparable control mix are available in Appendix A, Table 10.

Table 8

Mixture Proportions of Ternary Blended Concrete Per Cubic Yard

	PC77.5FAF12.5GGBFS10 Mix 1	PC72.5FAC25SF2.5 Mix 2	PC77.5FAC12.5GGBFS10 Mix 3
Cement, lb	344.7	415.8	405.3
Fly Ash, lb	74.9	148.5	90.1
Slag, lb	179.9	-	105.1
Silica Fume, lb	-	29.7	-
Water, lb	269.8	267.3	270.2
Sand, lb	1459.2	1459.2	1459.2
Nat. Agg., lb	1542.8	1542.8	1542.7
AEA, fl oz/cwt	1.8	2.2	2

Fresh and hardened mixture properties were recorded for each of the three blends. All hardened tests were conducted in triplicate and average values are presented. Full tabulated data is available in Appendix A. Table 9 shows the recorded fresh mixture properties for each of these concrete blends. Slump and air content were maintained for all blends. This indicated that none of the proposed ternary blends have a significant detrimental effect on workability or air content. Table 9 also provides data recorded with an air voids analyzer (AVA). In addition to calculation air content, the test also calculates specific surface, a ratio of surface area to volume, and spacing factor, or the maximum distance to an air void in the matrix. Due to the stiffness of the mixtures, samples were not necessarily fully broken apart by the stirring mechanism.

Table 9

Ternary Blended Concrete Fresh Properties

	PC77.5FAF12.5 GGBFS10	PC72.5FAC25 SF2.5	PC77.5FAC12.5 GGBFS10
Slump (in)	1.0	1.5	1.25
Air Content, %	5.50	5.50	5.00
Unit Wt. (pcf)	148.36	148.66	143.60
Mix temp (°F)	65	65	65
Air Void Analyzer			
Air-% Concrete	2.3	3.1	2.9
Specific Surface (in^{-1})	432	401	485
Spacing Factor (in)	0.0197	0.0186	0.0193

Figures 15, 16 and 17 provide evolution of strength, electrical resistivity, and alkali-silica reaction for each blend. All mixtures have similar late-age strength and resistivity values. PC77.5FAC12.5GGBFS10 had the slowest strength gain trend, however ultimately all mixtures performed nearly identical. While these mixes performed similarly in mortar testing, some factors are considered which may have caused more similarities in concrete mixing. First, concrete cylinders were mixed in a drum mixer, which has higher mixing energy than the process used to mix mortar cubes, which may have influenced mix properties. Additionally, the inclusion of coarse aggregates introduces additional interfacial transition zones and anisotropy to the mix which controls failure behavior more so than binder in the case where binders are relatively similar in strength. Likewise, alkali-silica reactivity is similar for all mixtures. ASR testing was conducted to 30 days to assess late-age trends in reactivity beyond specification. At up to 30 days, all samples maintained low-risk compliancy. Ultimately to select a blend to

proceed forward with in RCA testing the mortar cube analysis is considered. It was decided that PC77.5FAC12.5GGBFS10 was the optimal ternary binder blend based on higher predicted strength values from the mortar tests.

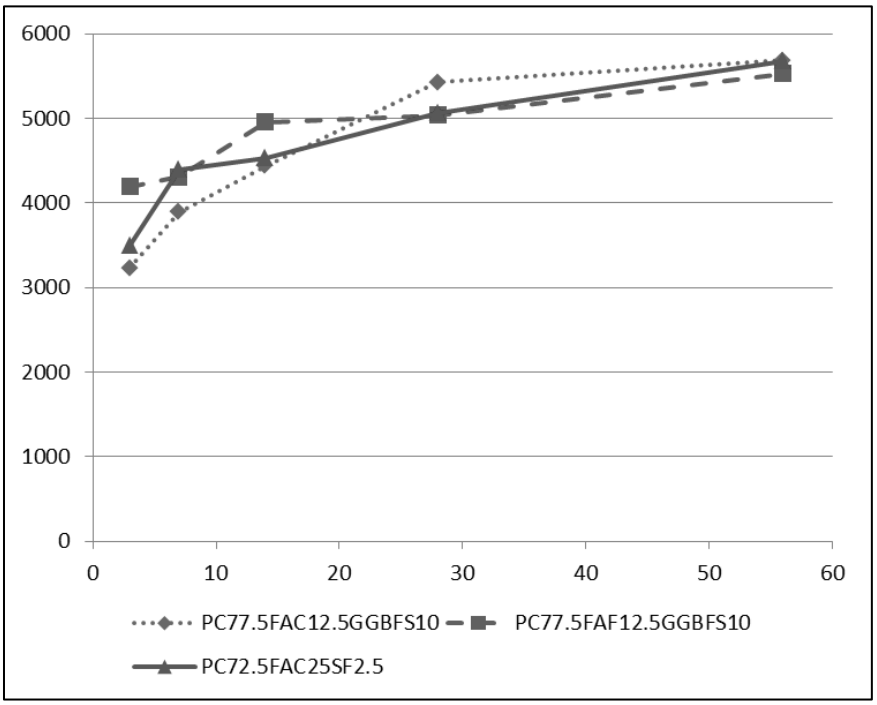

Figure 15. Ternary blended concrete compressive strength.

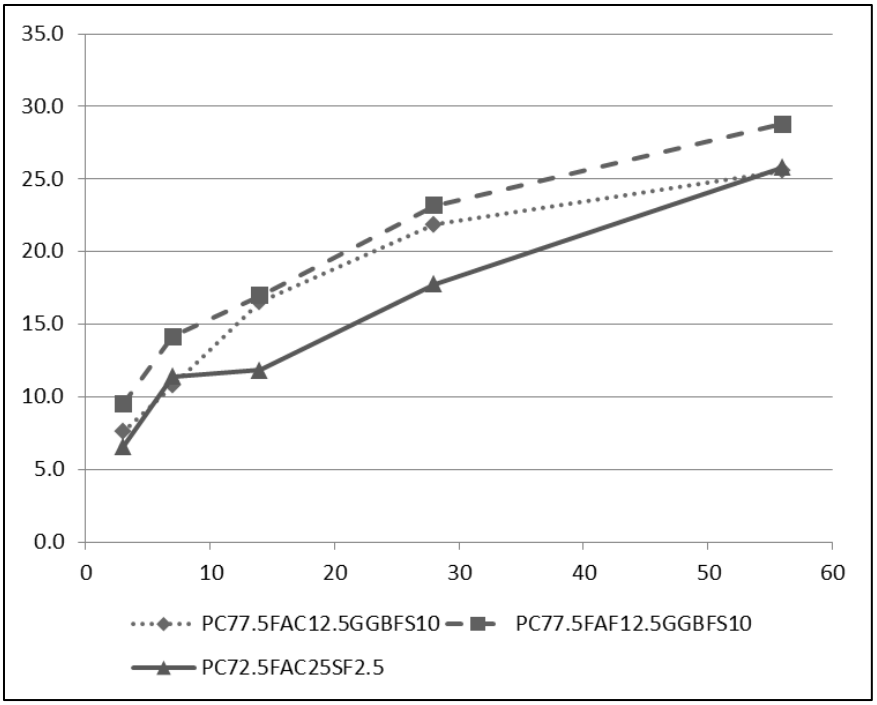

Figure 16. Ternary blended concrete electrical resistivity.

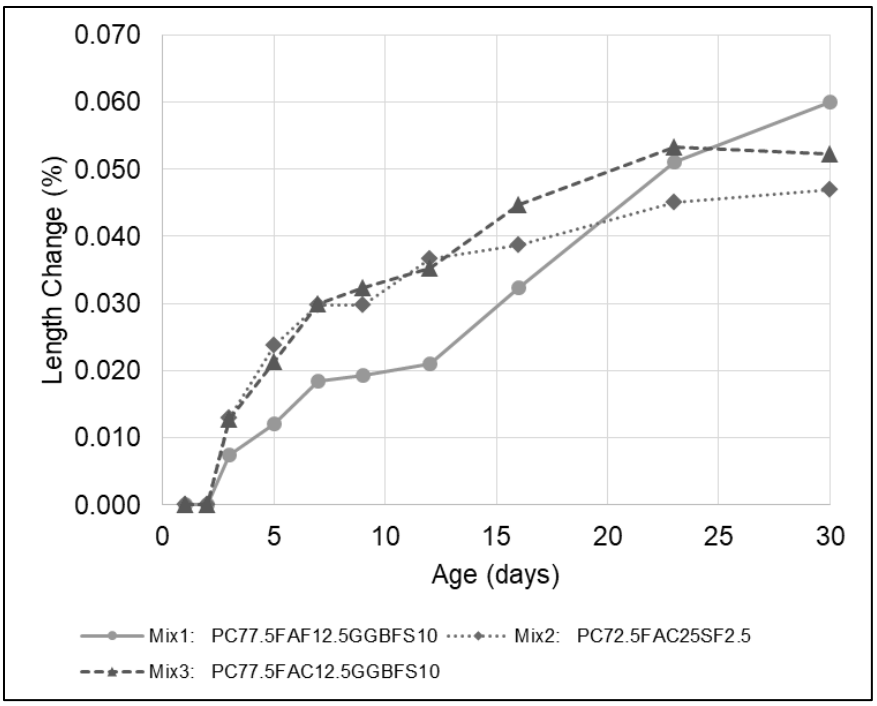

Figure 17. Ternary blended concrete alkali-silica reaction.

Ternary Blended Concrete with RCA Replacement

Table 10 shows proportions per cubic yard for each mixture with and without RCA and SCM. In this table, NC is used to describe the control mix with only virgin aggregates and portland cement binder. NC30 indicates that 30% of the coarse aggregate of the mix was replaced with RCA. NC30T indicates that the ternary blended binder was then implemented for the third iteration at 30% RCA. NC50T indicates that recycled aggregate content was then increased to 50%. Table 11 gives fresh properties recorded. For all mixes, slump was maintained at 25 millimeters ± 6 millimeters. Air content met or exceeded the target of 6% +2/-1 in all mixtures. AVA analysis indicated much lower air content, however it was noted that for all AVA tests the mortar samples were not properly broken apart during mechanical stirring. There was a slight pattern of loss of slump with increasing RCA replacement rate. This may be in part due to an increased mixing temperature as well as recycled aggregate porosity requiring more water. A higher dose of water reducer was required to counteract loss of slump at constant water content across all mixtures. The increase in RCA content also increased air content and reduced mixture unit weight.

Table 10

Ternary Blended RCA Mixture Proportions

	NC	NC30	NC30T	NC50T
Cement, lb	656	656	502.3	502.3
Fly Ash C, lb	-	-	81	81
Slag, lb	-	-	64.8	64.8
Water, lb	262.4	262.4	259.3	259.3
Sand, lb	1455	1455	1455.4	1455.4
Natural Agg, lb	1539	1077	1077.1	769.4
RCA, lb	-	415	415	691.6
AEA, fl oz/cwt	4	4	4	4
HRWR, fl oz/cwt	-	2.9	3.05	6.75

Figure 18 shows the progression of setting for each mixture. There is a clear increase in setting time of approximately 45-minutes to an hour when supplementary cementitious materials are included in the binder.

Table 11

Ternary Blended RCA Fresh Properties

	NC	NC30	NC30T	NC50T
Slump (in)	1.25	1.0	1.0	0.75
Air Content, %	6.0	6.0	6.0	7.0
Unit Wt. (pcf)	145	146	146	142
Mix temp (°F)	76	77	75	87
Air Void Analyzer				
Air-% Concrete	1.1	1.5	1.9	3.1
Specific Surface (in^{-1})	330.20	236.22	322.58	294.64
Spacing Factor (in)	0.0346	0.0433	0.0255	0.0241
Setting Time				
Initial (hrs:min)	3:30	3:20	5:15	4:55
Final (hrs:min)	5:15	5:10	6:35	6:30

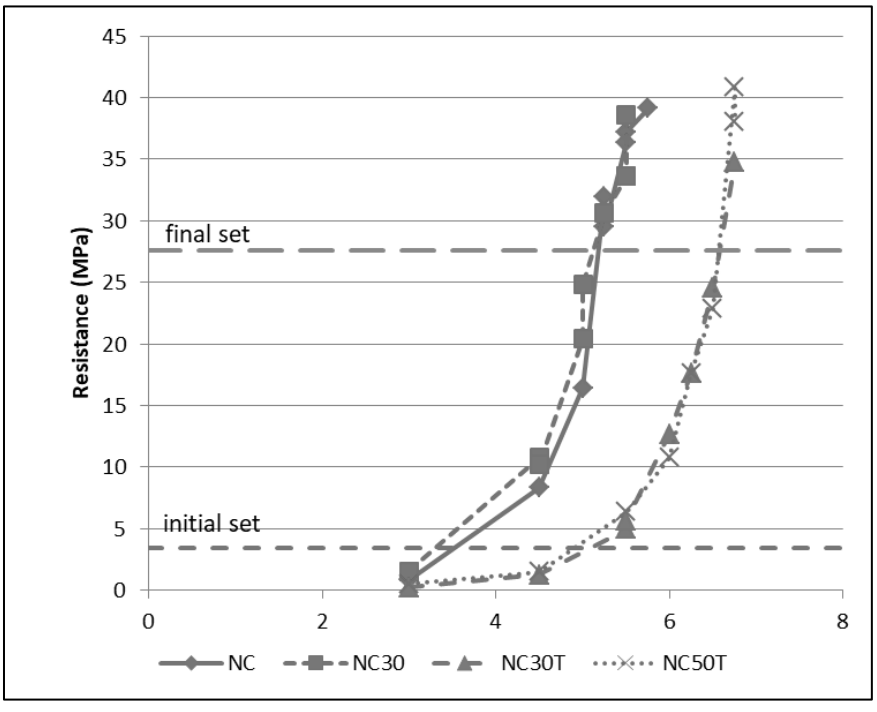

Figure 18. Ternary blended RCA setting time.

Trends in hardened properties for each mixture were also observed. All tabulated data is available in Appendix A. Compressive strength is shown in Figure 19. There is an increase in compressive strength at up to 50% recycled aggregate replacement. In all cases, mixtures including recycled aggregates exceed the control strength. At 30% replacement, the ternary blended mixture reduced early strength. However, late-age strength appears to increase beyond 56-days in ternary blends. Figure 20 shows results for elastic modulus. Modulus is similar for all blends at late age, however at 50% RCA the mixture developed more slowly. Modulus developed most quickly in the control blend but does not ultimately exceed the other blends.

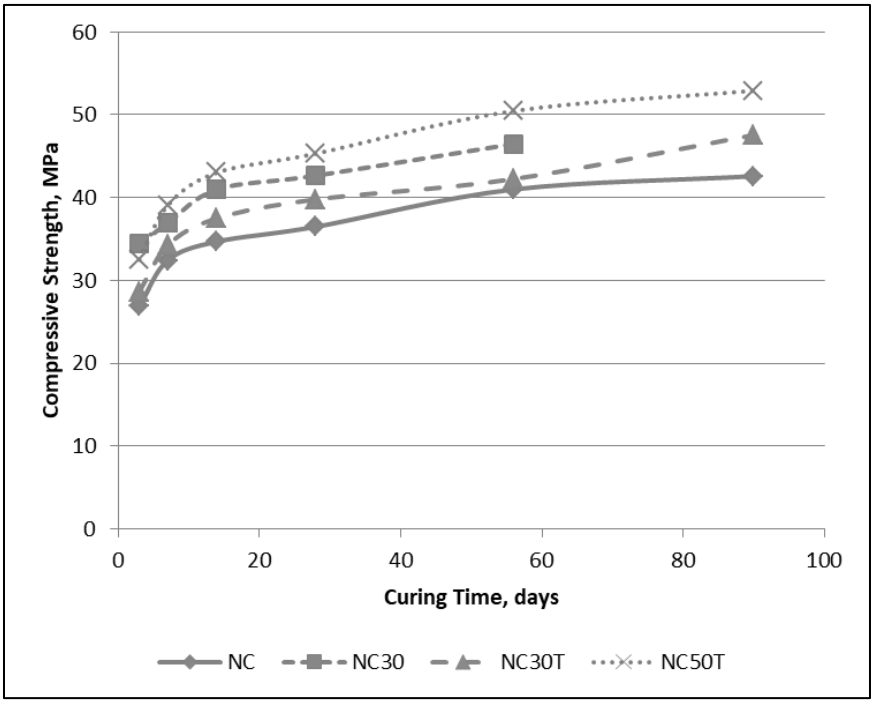

Figure 19. Ternary blended RCA compressive strength.

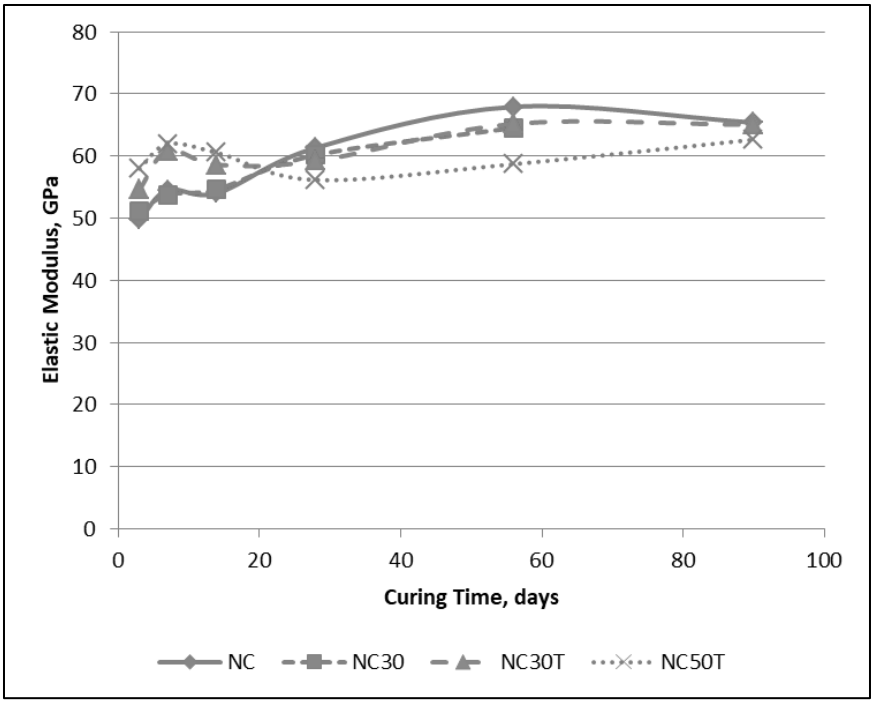

Figure 20. Ternary blended RCA Elastic Modulus.

Modulus of rupture at 28-days and 90-days is shown in Figure 21. In all cases, mixtures with RCA replacement had greater performance than the control. At 90-days, both mixtures with SCM had higher modulus of rupture than either the control or the 30% RCA mixture without mineral admixtures.

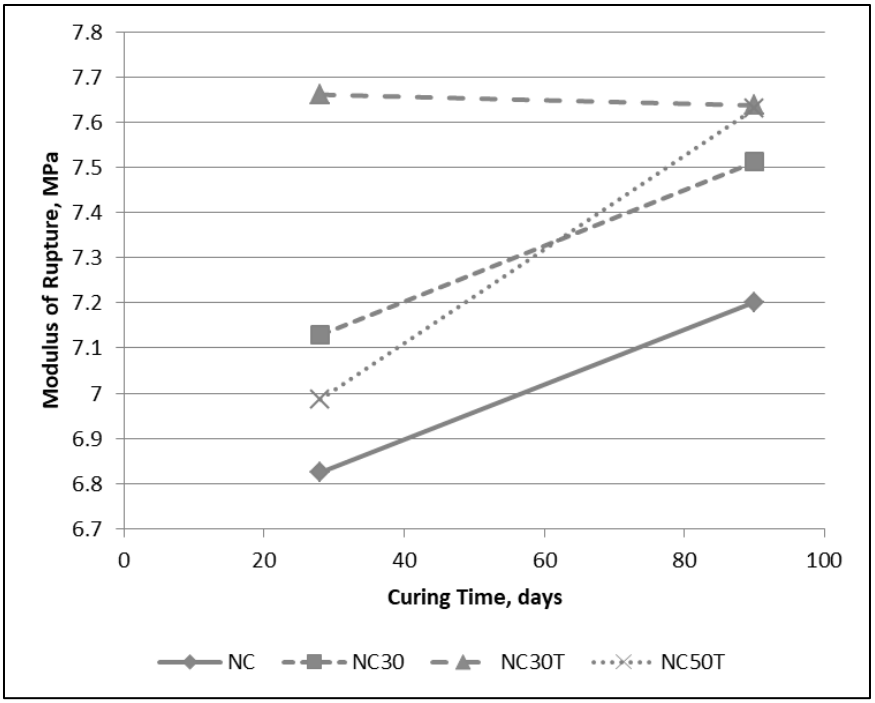

Figure 21. Ternary blended RCA modulus of rupture.

Electrical resistivity development is show in Figure 22. At 28-days, the control mixture maintains higher surface resistivity than the 30% RCA mixture. However, surface resistivity is improved in both ternary blended mixtures. NC30T (30% RCA, ternary blended) performed best, indicating that RCA had a negative effect on the surface resistivity of the mixtures and that the addition of SCM counteract this effect. Figure 23 shows data for drying shrinkage for all mixtures. The control blend showed the least change in length for the duration of testing. NC30 (30% RCA) showed the highest change in length. Again, this indicates that RCA replacement may increase drying shrinkage, however the use of SCM may alleviate this somewhat. As a measure of surface permeability, electrical resistivity should correlate with drying shrinkage. Higher permeability enables more surface drying due to climate exposure. This trend is observed

for tested samples. Figure 24 shows freeze-thaw durability testing for all mixtures. All mixtures reached 300 freeze-thaw cycles while maintaining relative dynamic modulus above 0.95.

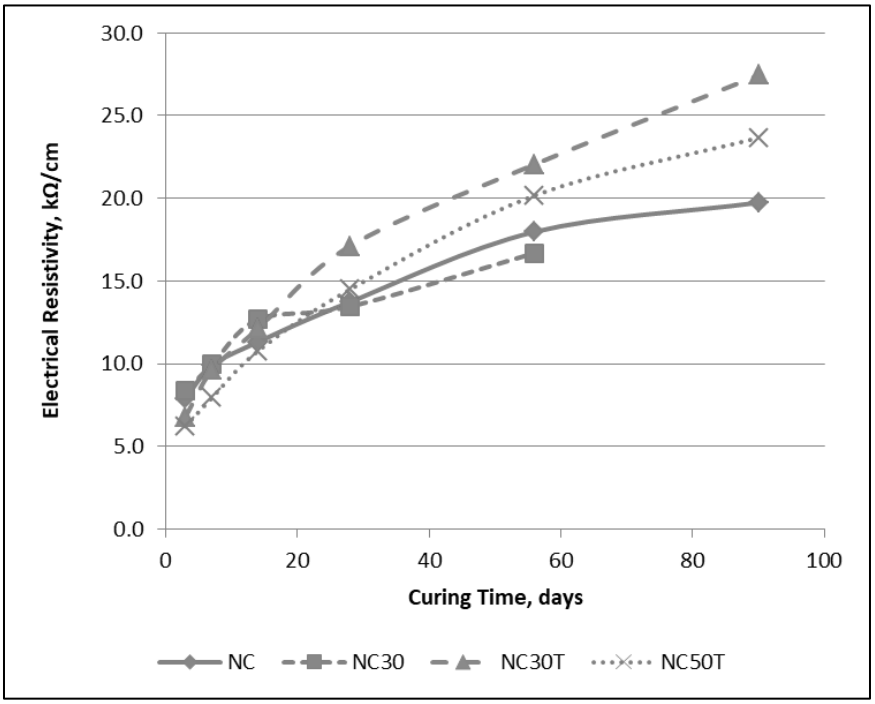

Figure 22. Ternary blended RCA surface resistivity.

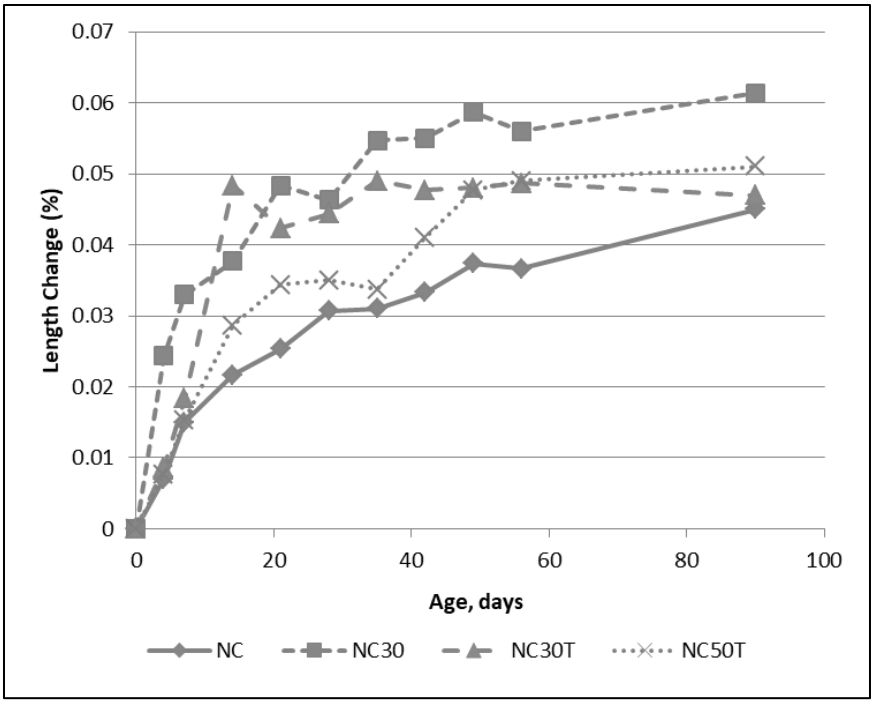

Figure 23. Ternary blended RCA drying shrinkage.

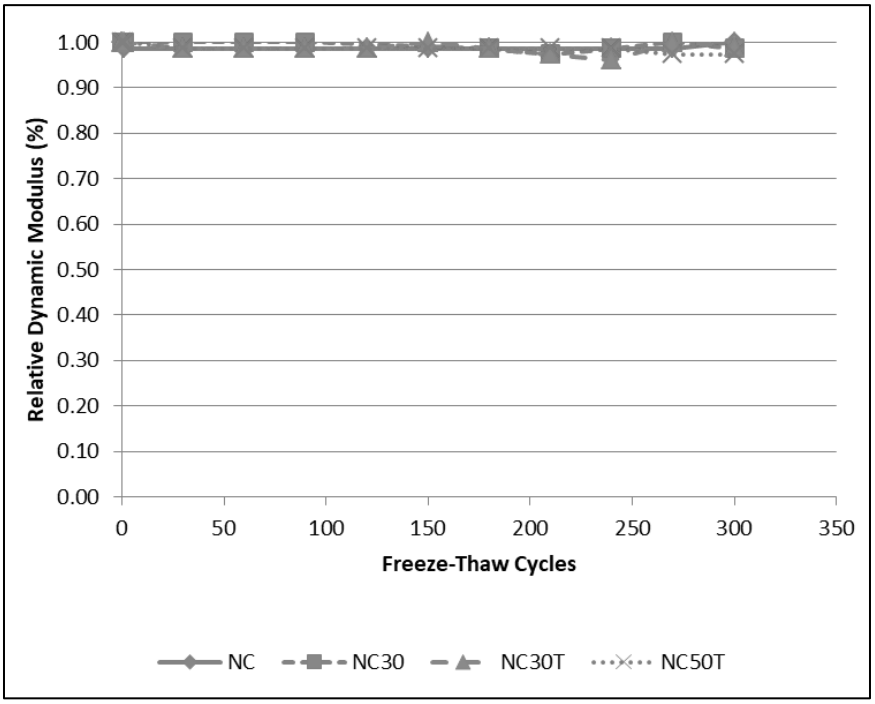

Figure 24. Ternary blended RCA freeze-thaw durability.

Alkali-silica reactivity for each mixture is presented in Figure 25. Length change over time increased with higher replacement rates of RCA. There was little difference in results between ternary blended mixtures and mixtures including only portland cement. At 50% RCA replacement, the samples failed to meet the 16-day low risk limit for length change (0.10%). The Class F fly ash and slag blend, PC72.7FAF12.5GGBFS10 was then tested at 50% replacement to analyze the effect of using a different binder (NC50Tb). As previously shown, this blend performed very similarly to the chosen ternary binder blend in compressive strength, resistivity, and alkali-silica reactivity in mixtures without RCA. The alternate blend had similar ASR to the control mixture. It is theorized that the Class F fly ash used may have contained less alkali content than the Class C (equivalent alkali content above 5%), and therefore lessened ASR when a more reactive aggregate was included. Equivalent alkali content is calculated as the sum of sodium oxide and potassium oxide compounds in the sample.

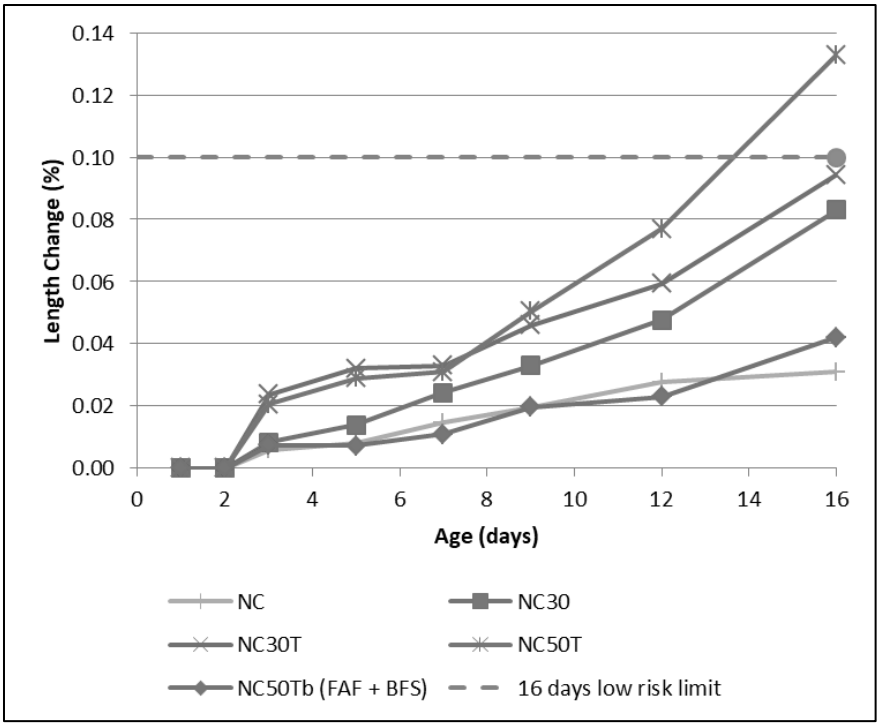

Figure 25. Ternary blended RCA ASR.

Chapter 6

Summary and Conclusions

Four ternary blended cement binders were analyzed at different proportions in order to optimize a concrete binder blend for the purpose of concrete strength. These were as follows: Class C fly ash and silica fume, Class C fly ash and ground granulated blast furnace slag (GGBFS), Class F fly ash and silica fume, Class F fly ash and GGBFS. Mortar cube compressive strength was recorded at 28 and 56 days for 25 unique cement blends varying mineral admixture replacement rate from 0% to 55% of binder by weight. Isothermal calorimetry was used to identify curing properties for each blend by analyzing thermal activity and hydration heat for each blend. Concrete compressive testing and statistical analysis concluded that a blend of 77.5% portland cement, 12.5% Class C fly ash, and 10% slag will produce the best compressive strengths among ternary blends without a loss in surface resistivity or alkali-silica reaction resistance.

Summary of Findings

1. Ternary combinations with Class C fly ash produced higher strengths than portland cement up to 55% total replacement with SCM at 56-days.
2. Ternary combinations with Class F fly and slag produced higher or similar strengths to portland cement when replacement is up to 57.5% at 56-days.
3. Ternary combinations of 12.5% Class F fly ash with 5% silica fume may produce strengths higher than PC at 56 days, but 5% silica fume alone with portland cement produced higher strength than the ternary blend.
4. The use of SCM tend to reduce the main peak in the heat of hydration, and the total amount of heat measured in the first 72 hours of hydration. Class C fly ash and slag had a

strong secondary C_3A reaction which may produce heat greater than the main C_3S and C_2S peak.

5. There was a consistent trend of reduced heat of hydration for ternary blended cements in the first 72-hours of hydration. The optimum strength with the low heat of hydration was replacement of portland cement with 25% Class C fly ash and 2.5% silica fume, while the ternary blend with the highest compressive strength was replacement with 12.5% Class C fly ash and 10% slag.

6. Less than 55% portland cement in a ternary blend lead to a decrease in mean strength compared to 100% portland cement strength at 56-days.

7. Flexural strength improved at up to 30% RCA use. The proposed ternary blended binder improved 90-day flexural strength above the portland cement mixtures.

8. 25 millimeters ± 25 millimeters slump and 6% +2/-1% air content were consistently achieved with the proposed mix design for all iterations of binder implementation and RCA replacement studied.

9. Surface resistivity decreased, drying shrinkage increased, and alkali-silica reaction increased with RCA use. However, the proposed ternary blended binder improved concrete performance in these tests.

Conclusions

Concrete mixtures were tested with increasing replacement rate of coarse aggregates by recycled concrete coarse aggregate and with the optimized ternary blended binder proportions. Fresh concrete properties were collected to check consistency of workability and air content between mixtures. Hardened concrete properties were analyzed up to 90-

days to compare the strength, durability, and resistance to chemical attack of each mixture. The following conclusions are drawn from this study.

1. For use in concrete with a fraction of recycled coarse aggregates, a binder proportion of 77.5% Type I portland cement, 12.5% Class C fly ash, and 10% ground granulated blast furnace slag proved to be optimal with respect to concrete strength, surface resistivity, and the limiting of drying shrinkage and alkali-silica reaction.

3. Screened and graded recycled concrete aggregate may be used in concrete mixtures at up to a 50% fraction of the coarse material without detriment to the strength, modulus, or durability of the concrete.

4. The porosity of RCA necessitated presoaking prior to batching as well as the potential use of workability-improving admixture to maintain consistent fresh mix workability at high coarse aggregate replacement by RCA.

5. The use of supplementary cementitious materials increased setting time consistently across trials. This has logistical application however may require additional planning to account for an additional 80 minutes to set time over portland cement mixtures.

6. Proper air entrainment (6% +2 -1 air voids) was sufficient to ensure marginal loss of freeze-thaw durability characteristics at 50% RCA use.

7. Durability characteristics were properly controlled at 50% RCA with the incorporation of the optimized ternary blended binder.

Future Work

This study proves the utility of ternary blended binders applied in concrete mixtures which use recycled concrete coarse aggregates. The following are recommended as additional avenues of research following this study.

1. This study addresses the use of Class C fly ash, Class F fly ash, silica fume, and ground granulated blast furnace slag. There are several mineral admixtures commonly used which may be examined via similar experimentation which include limestone, metakaolin, etc.
2. Higher replacement rates of RCA may be tested. In this study, the detrimental effects of RCA (shrinkage, resistivity, ASR) are controlled at up to 50%. There exists the potential for successful concrete mixtures that incorporate up to 100% coarse RCA replacement.
3. This study addresses the incorporation of RCA that was collected from a single source. Due to the variability of RCA, additional RCA sources of varying qualities may be tested.
4. Different sources of RCA will have varying strength and durability characteristics. With the testing of many sources of RCA, unified guidelines for the use of RCA based on aggregate quality as it relates to the tests conducted in this study may be designed.

References

[1] J.F. Lamond, R.L. Campbell Sr., T.R. Campbell, J.A. Cazares, A. Giraldi, W. Halczak, H.C. Hale Jr., N.J.T. Jenkins, R. Miller, and P.T. Seabrook. (2001). "Removal and Reuse of Hardened Concrete." ACI Committee 555. ACI 555R-01.

[2] D. Pedro, L. de Brito, and L. Evangelista. (2014). "Influence of the use of recycled concrete aggregates from different sources on structural concrete." Elsevier. Construction and Building Materials. 71, pp. 141-151.

[3] M.S. Meddah. (2016). "Recycled aggregates in concrete production: engineering properties and environmental impact." MATEC. Web of Conferences. 101, 05021.

[4] ACPA (2010). "Why Recycle Concrete Pavements?" Concrete Pavement Technology Series, TS043, pp. 1. Skokie, IL.

[5] ACPA (2010). "Properties and Characteristics of CCCA." Concrete Pavement Technology Series, TS043, pp. 5. Skokie, IL.

[6] A. Abbaspour, B.F. Tanyu, and B. Cetin. (2016). "Impact of Aging on Leaching Characteristics of Recycled Concrete Aggregate." Environmental Science and Pollution Research. 23:20835–20852.

[7] C.-S. Poon, X. C. Qiao, and D. Chan. (2006). "The Cause and Influence of Self-Cementing Properties of Fine Recycled Concrete Aggregates on the Properties of Unbound Sub-Base." Waste Management, 26 (10), pp. 1166-1172.

[8] J. McIntyre, S. Spatari, and H. L. MacLean. (2009). "Energy and Greenhouse Gas Emissions Trade-Offs of Recycled Concrete Aggregate Use in Nonstructural Concrete: A North American Case Study." ASCE Journal of Infrastructure Systems, Dec. 2009. pp. 361-370.

[9] M.J. McGinnis, M. Davis, A. de la Rosa, B.D. Weldon, and Y.C. Kurama. (2017). "Quantified Sustainability of Recycled Concrete Aggregates." Institution of Civil Engineers. Magazine of Concrete Research, Paper 1600338.

[10] ASTM C29/C29M-17a, Standard Test Method for Bulk Density ("Unit Weight") and Voids in Aggregate, ASTM International, West Conshohocken, PA, 2015, www.astm.org.

[11] S. H. Kosmatka, B. Kerkhoff and W. C. Panarese. (2002). "Design and Control of Concrete Mixtures." Skokie:Portland Cement Association.

[12] M. C. Limbachiya, T. Leelawat and R. K. Dhir. (2000). "Use of Recycled Concrete Aggregate in High-Strength Concrete." Materials and Structures, 33 (233), pp. 574-580.

References (Continued)

[13] N. K. Bairagi, K. Ravande and V. K. Pareek. (1993). "Behaviour of Concrete with Different Proportions of Natural and Recycled Aggregate." Resources, Conservation and Recycling, 9 (1-2), pp. 109-126.

[14] L. Butler, J. S. West and S. L. Tighe. (2011). "The Effect of Recycled Concrete Aggregate Properties on the Bond Strength Between CCCA Concrete and Steel Reinforcement." Cement and Concrete Research, 41 (10), pp. 1037-1049.

[15] ASTM C29/C29M, Standard Test Method for Bulk Density ("Unit Weight") and Voids in Aggregate, ASTM International, West Conshohocken, PA, 2017, www.astm.org.

[16] ASTM C131/C131M-14, Standard Test Method for Resistance to Degradation of Small-Size Coarse Aggregate by Abrasion and Impact in the Los Angeles Machine, ASTM International, West Conshohocken, PA, 2017, 2006, www.astm.org.

[17] M. A. Berube, J. Frenette and B. Marquis. (2002). "Frost-Resistance of Concrete Incorporating Coarse Aggregates Made of Recycled Concrete." in Proceedings, Annual Conference - Canadian Society for Civil Engineering.

[18] ASTM C136/C136M-14, Standard Test Method for Sieve Analysis of Fine and Coarse Aggregates, ASTM International, West Conshohocken, PA, 2014, www.astm.org.

[19] ASTM D4791 – 10, Standard Test Method for Flat Particles, Elongated Particles, or Flat and Elongated Particles in Coarse Aggregate, ASTM International, West Conshohocken, PA, 2010, www.astm.org.

[20] K.W. Anderson, J.S. Uhlmeyer, and M Russell. (2009). "Use of Recycled Concrete Aggregate in PCCP: Literature Search." Washington State Department of Transportation. Special Report.

[21] D.B. Cleary. (2013). "Recycled Concrete Aggregate in Portland Cement Concrete." Rowan University. NJDOT Final Report.

[22] (2007). New Jersey Department of Transportation Standard Specifications for Road and Bridge Construction. NJDOT. Table 901.10.02-1, pp. 321.

[23] ACI Committee 221 (2001). "Guide for Use of Normal Weight and Heavyweight Aggregates in Concrete." ACI Committee 221. ACI 221R-96.

[24] ASTM C143 / C143M-15a, Standard Test Method for Slump of Hydraulic-Cement Concrete, ASTM International, West Conshohocken, PA, 2015, www.astm.org.

References (Continued)

[25] M. Barra, M. Etxeberria, A. Marí, and E. Vázquez. (2007). "Influence of Amount of Recycled Coarse Aggregates and Production Process on Properties of Recycled Aggregate Concrete." Cement and Concrete Res., 37 (5), pp. 735-742.

[26] T. Brown, K.K. Sagoe-Crentsil, and A.H. Taylor. (2001). "Performance of Concrete Made With Commercially Produced Coarse Recycled Concrete Aggregate." Cement Concrete Res., 31(5), pp. 707-712.

[27] B. Bissonnette, D. Burns, F. Gagnon, M. Jolin, and L. Bolduc. (2009) "Understanding the Pumpability of Concrete." Shotcrete for Underground Support XI.

[28] Hallet, Bernard. (2006). "Why Do Freezing Rocks Break?" Science, 314 (5802), pp. 1092–1093.

[29] M.S. Mamlouk, and J.P. Zaniewski. (2011). Materials for Civil and Construction Engineers, third edition. Upper Saddle River, NJ.

[30] S.R. Boyle, D.I. McLean, D.G. Mjelde, T.C. Spry, and H. Wen. (2014). "Evaluation of Recycled Concrete as Aggregate in New Concrete Pavements." Research Project T4120-32 Evaluation of Recycled Concrete. Dept. of Transportation, Olympia, WA.

[31] P. Amorim, J. de Brito, and L. Evangelista. (2012). "Concrete Made with Coarse Concrete Aggregate: Influence of Curing on Durability." ACI Mater J, 109 (2).

[32] S. Desai. (2004). "Appreciation of Risks in Specifying and Designing Concrete Structures," Building Engineer, 79 (6), pp. 26-29.

[33] S. B. Desai and M. C. Limbachiya. (2006). "Coarse Recycled Aggregate - A Sustainable Concrete Solution." Indian Concrete Journal, 80 (7), pp. 17-23.

[34] M. Davis, A. de la Rosa, Y. Kurama, and M. McGinnis. (2017). "Strength and Stiffness of Concrete with Recycled Concrete Aggregates." Construction and Building Materials, 154, pp. 258-269.

[35] M. Hayles, F. Ahimoghadam, L. Sanchez, and M. Noel. (2017) "Effect of Original Concrete Properties on Performance of CCCA Concrete." Presented at ACI October 2017.

[36] A.S. Abdel-Hay. (2015). "Properties of Recycled Concrete Aggregate Under Different Curing Conditions." Housing and Building National Research Center, 2-6.

References (Continued)

[37] V. Corinaldesi (2010). “Mechanical and Elastic Behavior of Concrete Made of Recycled-Concrete Coarse Aggregate.” Construction and Building Materials 24, pp. 1616-1620.

[38] ASTM, ASTM C469 / C469M - 10 Standard Test Method for Static Modulus of Elasticity and Poisson's Ratio of Concrete in Compression, Conshohocken, PA, www.astm.org.

[39] U. Meinhold, G. Mellmann, and M. Maultzsch. (2001). "Performance of High-Grade Concrete with Full Substitution of Aggregates by Recycled Concrete." in SP-202: Third Canmet/ACI International Symposium: Sustainable Development of Cement and Concrete.

[40] V. W. Y. Tam, C. M. Tam and Y. Wang. (2007) "Optimization on Proportion for Recycled Aggregate in Concrete Using Two-Stage Mixing Approach," Construction and Building Materials, 21 (10), pp. 1928-1939.

[41] S. C. Kou, C. S. Poon and C. Dixon, "Influence of Fly Ash as Cement Replacement on the Properties of Recycled Aggregate Concrete," Journal of Materials in Civil Engineering, 19 (9), pp. 709-717, 2007.

[42] K.Y. Ann, Y.B. Kim, H.Y. Moon, and J. Ryou. (2007). “Durability of Recycled Concrete Using Pozzolanic Materials.” Waste Management, 28, pp. 993-999.

[43] S.C. Angulo, B. Cazacliu, A. Cothenet, E. Hamard, and M. Quattrone. (2016). “Measuring the Water Absorption of Recycled Aggregates, What is the Best Practice for Concrete Production?” Construction and Building Materials, 123, pp. 690-703.

[44] ASTM C642-13, Standard Test Method for Density, Absorption, and Voids in Hardened Concrete, ASTM International, West Conshohocken, PA, 2013, www.astm.org.

[45] ASTM D4404-10, Standard Test Method for Determination of Pore Volume and Pore Volume Distribution of Soil and Rock by Mercury Intrusion Porosimetry, ASTM International, West Conshohocken, PA, 2010, www.astm.org.

[46] T.C. Hansen. (1986). “Recycled Aggregates and Recycled Aggregate Concrete Second State-of-the-Art Report Developments 1945-1985.” Materials and Structures, 1 (111), pp. 201-246.

[47] C. Thomas, J. Setién, J.A. Polanco. P. Alaejos, and M. Sánchez De Juan. (2013). “Durability of Recycled Aggregate Concrete.” Construction and Building Materials, 40, pp. 1054-1065.

References (Continued)

[48] J. Andal, M. Shehata, and P. Zacarias. (2016). “Properties of Concrete Containing Recycled Concrete Aggregate of Preserved Quality.” Construction and Building Materials, 125, pp. 842-855.

[49] J-Z. Xiao, X-D. Xu, and Y-H. Fan. (2013). “Shrinkage and creep of recycled aggregate concrete and their prediction by ANN method.” Journal of Building Materials, 16 (5), pp. 752-757.

[50] T. Yamato, Y. Emoto, and M. Soeda. (1998). “Mechanical Properties, Drying Shrinkage and Resistance to Freezing and Thawing of Concrete Using Recycled Aggregate.” American Concrete Institute. ACI Special Publication SP 179-7, 179 pp. 105-122.

[51] ASTM C596-09, Standard Test Method for Drying Shrinkage of Mortar Containing Hydraulic Cement, ASTM International, West Conshohocken, PA, 2017, www.astm.org

[52] ASTM, ASTM C666 (2012b), Standard test method for resistance of concrete to rapid freezing and thawing, Conshohocken, PA, www.astm.org.

[53] J. Yamasaki and K. Tatematsu. (1998). “Strength and Freeze-Thaw Resistance Properties of Concrete Using High-Quality Recycled Aggregate.” Asanuma Corp. Japan. Transactions of the Japan Concrete Institute, 20, pp. 45-52.

[54] R. M. Salem, E. G. Burdette and N. M. Jackson. (2003). "Resistance to Freezing and Thawing of Recycled Aggregate Concrete." ACI Materials Journal, 100 (3), pp. 216-221.

[55] Y. Wei, Y. Meng and Q. Sun. (2012). "Effects of Calcined Diatomite on Resistance to Permeability and Freeze-Thaw of Recycled Aggregate Concrete (RAC)." 2nd International Conference on Frontiers in Manufacturing and Design Science.

[56] S.B. Huda and M.S. Alam. (2015). “Mechanical and Freeze-Thaw Durability Properties of Recycled Aggregate Concrete Made with Recycled Coarse Aggregate.” Journal of Materials in Civil Engineering, 27 (10).

[57] N.S. Amorim, Jr., G.A.O. Silva, and D.V. Ribeiro. (2017). “Effects of the Incorporation of Recycled Aggregate in the Durability of the Concrete Submitted to Freeze-Thaw Cycles.” Construction and Building Materials.

[58] K. Obla. (2005). “Alkali Silica Reactions.” Concrete in Focus. Naylor Publications, Inc. Silver Spring, Md. pp. 45-47.

References (Continued)

[59] ASTM C 1293, Standard Test Method for Determination of Length Change of Concrete Due to Alkali-Silica Reaction, ASTM International, West Conshohocken, PA, 2015, www.astm.org.

[60] X. Li and D.L. Gress. (2006). "Mitigating Alkali-Silica Reaction in Concrete Containing Recycled Concrete Aggregate." Transportation Research Record, 1979, pp. 30-35.

[61] M.D.A. Thomas, B. Fournier, K.J. Folliard. (2008). "Report on Determining the Reactivity of Concrete Aggregates and Selecting Appropriate Measures for Preventing Deleterious Expansion in New Concrete Construction." The Transtec Group, Inc. Austin, Tx.

[62] United States of America Department of Defense. (2004). Standard Practice for Concrete Pavements. UFC 3-250-04 pp. 4.

[63] United States of America Department of Defense. (2004). Standard Practice for Pavement Recycling. UFC 3-250-07 pp. (5-1)-(5-3).

[64] United States of America Department of Defense. (2011). Portland Cement Concrete Pavement for Roads and Site Facilities. USACE Unified Facilities Guide Specifications, UFGS-32 13 13.06.

[65] United States of America Department of Defense. (2015). Concrete Pavement for Airfields and Other Heavy-Duty Pavements. USACE Unified Facilities Guide Specifications, UFGS-32 13 11.

[66] United States of America Department of Defense. (2017). Aggregate Base Courses. USACE Unified Facilities Guide Specifications, UFGS-32 11 23.

[67] United States of America Department of Defense. (2007). Engineering Technical Letter (ETL) 07-6: Risk Assessment Procedure for Recycling Portland Cement Concrete (PCC) Suffering from Alkali-Silica Reaction (ASR) in Airfield Pavement Structures. HQ AFCESA/CEOA, ETL-07-6.

[68] United States of America Department of Defense. (2006). Lean Concrete Base Course. USACE Unified Facilities Guide Specifications, UFGS-32 11 36.13.

[69] P. Ghosh, S. Hanson, P. Taylor, P. Tikalsky, and K. Wang. (2011). "Development Of Performance Properties Of Ternary Mixtures: Laboratory Study On Concrete." Report No. DTFH61-06-H-00011, National Concrete Pavement Technology Center, Ames, IA.

References (Continued)

[70] S.G. Kim. (2010). "Effect of Heat Generation from Cement Hydration on Mass Concrete Placement." MS thesis. Iowa State University. pp. 14-20.

[71] K. Wang, Z. Ge, J. Grove, J. Mauricio Ruiz, and R. Rasmussen. (2006). "Developing a Simple and Rapid Test for Monitoring the Heat Evolution of Concrete Mixtures for Both Laboratory and Field Applications." Center for Transportation Research and Education, Iowa State University.

[72] J. Dewar. (2003). "Mix Design." Advanced Concrete Technology; Processes. Elsevier, Butterworth-Heinemann. Oxford, UK.

[73] ACI Committee 211. (2002). "Standard Practice for Selecting Proportions for Normal, Heavyweight, and Mass Concrete." ACI Committee 211. ACI 211.1-91.

[74] (2012). "5.3 Mix Design Methods." Construction Manual, 2012. Kansas DOT. pp. 1-7.

[75] M.E. Ayers, A. Davis, G.J. Fick, J. Gajda, J. Grove, D. Harrington, B. Kerkhoff, S.H. Kosmatka, H.C. Ozyildirim, J.M. Shilstone., K. Smith, S.M. Tarr, P.D. Tennis, P.C. Taylor, T.J. Van Dam, G.F. Voigt, and S. Waalkes. (2007). "Integrated Materials and Construction Practices for Concrete Pavement: A State-of-the-Practice Manual." Report No. FHWA HIF - 07 – 004, Federal Highway Administration, Washington, D.C.

[76] H Tutanji and T El-Korchi. (1995), "The influence of silica fume on the compressive strength of cement paste and mortar" Cement and Concrete Research, 25(7). pp 1592.

[77] ASTM C595 / C595M-17, Standard Specification for Blended Hydraulic Cements, ASTM International, West Conshohocken, PA, 2017, www.astm.org.

[78] C. Goguen. (2014). "Portland-Limestone Cement." (Online). Available: <http://precast.org/2014/06/portland-limestone-cement/> (Oct. 16, 2017).

[79] F. Bektas, H. Ceylan, P, Taylor, and E. Yurdakul. (2014), "Effect of Water-to-Binder Ratio, Air Content, and Type of Cementitious Materials on Fresh and Hardened Properties of Binary and Ternary Blended Concrete." Journal of Materials in Civil Engineering, 26 (60).

[80] A.R. Hariharan, A S Santhi, and G Mohan Ganesh. (2011), "Effect of Ternary Cementitious system on compressive strength and resistance to Chloride ion penetration" International Journal of Civil and Structural Engineering, 1 (4). (700-701).

References (Continued)

[81] R. Bleszynski, R.D. Hooton, M.D.A. Thomas, and C.A. Rogers. (2002) "Durability of Ternary Blend Concrete with Silica Fume and Blast-Furnace Slag: Laboratory and Outdoor Exposure Site Studies" ACI Materials Journal, 99 (5), pp. 499-508.

[82] X. Hu, C. Shi, X. Shi, B. Tong, and D. Wang. (2017) "Early Age Shrinkage and Heat of Hydration of Cement-Fly Ash-Slag Ternary Blends." Construction and Building Materials." 153, pp. 858-865.

[83] C.J. Stundebeck. (2007) "Durability of Ternary Blended Cements in Bridge Applications." University of Missouri-Columbia.

[84] H. Gurdián, E. García-Alcocel, F. Baeza-Brotons, P. Garcés, E. Zornoza. (2014). "Corrosion Behavior of Steel Reinforcement in Concrete with Recycled Aggregates, Fly Ash and Spent Cracking Catalyst." Materials, 7 (4) pp. 3176-3197.

[85] K. Kim, M. Shin, and S. Cha. (2013). "Combined Effects of Recycled Aggregate and Fly Ash Towards Concrete Sustainability." Construction and Building Materials, 48 pp. 499-507.

[86] S. Sadati, M. Arezoumandi, K.H. Khayat, and J.S. Volz. "Shear Performance of Reinforced Concrete Beams Incorporating Recycled Concrete Aggregate and High-Volume Fly Ash." J. Cleaner Product., 115 pp. 284-293.

[87] K. Cong. (2006). "Reusing Recycled Aggregates in Structural Concrete." PhD thesis. Hong Kong Polytechnic University/Civil Engineering. Hong Kong, China. pp. 278.

[88] M. Pepe. (2015). "A Conceptual Model For Designing Recycled Aggregate Concrete For Structural Applications." PhD thesis. University of Salerno/Civil Engineering. Italy. pp. 167.

[89] S. Kou, C. Poon. (2009). "Properties of Self-Compacting Concrete Prepared with Coarse and Fine Recycled Concrete Aggregates." Cement and Concrete Composites, vol. 31 no. 9, pp. 622-627.

[90] C. Lima, A. Caggiano, C. Faella, E. Martinelli, M. Pepe, and R. Realfonzo. (2013). "Physical Properties and Mechanical Behaviour of Concrete Made with Recycled Aggregates and Fly Ash." Construction Building Materials, 47 pp. 547-559.

[91] Y.V. Akbari and D. Rushabh. (2015). "Behavior of Recycled Coarse Aggregate in Ternary Blended Concrete with Microsilica and Flyash." International Journal for Scientific Research & Development. 3 (3).

References (Continued)

[92] Taylor, P. (2014). "The Use of Ternary Mixtures in Concrete." InTrans Project Reports. 74.

[93] Rupnow, T. D. "Evaluation of Ternary Cementitious Combinations." Louisiana Transportation Research Center, Baton Rouge, LA, 2012.

[94] S.G. Kim. "Effect of Heat Generation from Cement Hydration on Mass Concrete Placement." MS thesis. Iowa State University. 2010, pp. 14-20.

[95] Neville, A. M., Properties of Concrete, 4th ed. New York: John Wiley and Sons, 1996.

Appendix A

Additional Tabulated Data

Table A1

28-Day Mortar Cube Compressive Strength

Mixture	Compressive Strength, psi			Average	Standard Deviation
PC100	6839.30	6306.70	5996.10	6380.70	426.443
PC75FAC25	6482.70	7648.40	6980.30	7037.13	584.924
PC75FAF25	6384.50	5726.70	6208.80	6106.67	340.586
PC95SF5	6605.80	7379.10	6598.10	6861.00	448.704
PC70GGBFS30	5135.90	4564.60	6673.00	5457.83	1090.44
PC45FAC25GGBFS30	6052.10	6311.60	5733.80	6032.50	289.398
PC55FAC25GGBFS20	6779.10	7209.40	6852.10	6946.87	230.272
PC65FAC25GGBFS10	7025.70	7129.80	6842.10	6999.20	145.669
PC57.5FAC12.5GGBFS30	6837.30	7320.70	7095.60	7084.53	241.89
PC67.5FAC12.5GGBFS20	6830.50	7692.00	7247.10	7256.53	430.827
PC77.5FAC12.5GGBFS10	6436.10	6836.80	6984.70	6752.53	283.842
PC70FAC25SF5	6770.90	6987.10	6651.50	6803.17	170.111
PC72.5FAC25SF2.5	7676.30	8261.50	7367.00	7768.27	454.286
PC82.5FAC12.5SF5	6905.40	7040.10	6878.00	6941.17	86.7672
PC85FAC12.5SF2.5	7247.70	7074.70	7269.20	7197.20	106.631
PC45FAF25GGBFS30	5767.60	5366.10	5987.10	5706.93	314.914
PC55FAF25GGBFS20	5627.10	6059.10	5987.90	5891.37	231.614
PC65FAF25GGBFS10	5834.70	5716.30	3628.60	5059.87	1240.93
PC57.5FAF12.5GGBFS30	6840.30	6802.20	6752.90	6798.47	43.8194
PC67.5FAF12.5GGBFS20	6457.90	7339.30	6043.30	6613.50	661.863
PC77.5FAF12.5GGBFS10	6384.90	6475.40	6084.30	6314.87	204.74
PC70FAF25SF5	5822.10	6029.90	5803.50	5885.17	125.687
PC72.5FAF25SF2.5	5122.00	6099.70	6041.60	5754.43	548.473
PC82.5FAF12.5SF5	6298.00	6281.50	6787.20	6455.57	287.321
PC85FAF12.5SF2.5	5584.80	6627.50	6324.50	6178.93	536.375

Table A2

56-Day Mortar Cube Compressive Strength

Mixture	Compressive Strength, psi			Average	Standard Deviation
PC100	4508.40	6502.80	5199.00	5403.40	1012.79
PC75FAC25	6164.00	6074.70	5750.00	5996.23	217.869
PC75FAF25	4936.20	5049.10	5378.90	5121.40	230.035
PC95SF5	6324.30	6703.30	5666.20	6231.27	524.772
PC70GGBFS30	6480.40	6917.50	6654.30	6684.07	220.065
PC45FAC25GGBFS30	7241.30	6245.60	6558.40	6681.77	509.185
PC55FAC25GGBFS20	7718.40	7428.60	7494.40	7547.13	151.926
PC65FAC25GGBFS10	6519.20	7154.90	8426.60	7366.90	971.211
PC57.5FAC12.5GGBFS30	7353.70	7418.20	7715.20	7495.70	192.809
PC67.5FAC12.5GGBFS20	8356.20	7895.40	7639.80	7963.80	363.065
PC77.5FAC12.5GGBFS10	8084.20	7230.20	8305.40	7873.27	567.788
PC70FAC25SF5	7207.00	6996.60	6890.70	7031.43	161.001
PC72.5FAC25SF2.5	7915.80	7291.00	8831.60	8012.80	774.867
PC82.5FAC12.5SF5	7462.90	7620.60	6590.40	7224.63	554.893
PC85FAC12.5SF2.5	7160.30	8361.50	6693.20	7405.00	860.648
PC45FAF25GGBFS30	6356.60	6604.00	6317.50	6426.03	155.359
PC55FAF25GGBFS20	6309.30	6535.70	6605.60	6483.53	154.885
PC65FAF25GGBFS10	7116.30	6946.20	7017.30	7026.60	85.4305
PC57.5FAF12.5GGBFS30	7031.60	7235.30	7026.70	7097.87	119.046
PC67.5FAF12.5GGBFS20	7691.00	7911.20	6801.30	7467.83	587.641
PC77.5FAF12.5GGBFS10	7146.20	7138.60	7082.00	7122.27	35.0784
PC70FAF25SF5	6509.00	6781.80	6221.60	6504.13	280.132
PC72.5FAF25SF2.5	6493.10	7433.00	6573.40	6833.17	521.02
PC82.5FAF12.5SF5	7135.50	8068.70	6405.30	7203.17	833.762
PC85FAF12.5SF2.5	6889.90	7192.00	6635.60	6905.83	278.542

Table A3

Ternary Blended Concrete Hardened Properties

	PC77.5FAF12.5 GGBFS10	PC72.5FAC25SF2.5	PC77.5FAC12.5 GGBFS10
Compressive strength			
3d (psi)	4189	3493	3231
7d (psi)	4309	4396	3892
14d (psi)	4953	4535	4438
28d (psi)	5037	5061	5426
56d (psi)	5528	5659	5686
Electrical Resistivity			
3d (kΩ/cm)	9.5	6.6	7.6
7d (kΩ/cm)	14.1	11.4	10.8
14d (kΩ/cm)	17.0	11.8	16.5
28d (kΩ/cm)	23.2	17.8	21.9
56d (kΩ/cm)	25.6	25.8	25.1

Table A4

PC77.5FAC12.5GGBFS10 Ternary Blended Alkali-Silica Reaction

Time (days)	Std Bar RDG (in)	Specimen RDG (in)	CRD	ΔL_x (%)	Mass (lb)	Specimen RDG (in)	CRD	ΔL_x (%)	Mass (lb)	Specimen RDG (in)	CRD	ΔL_x (%)	Mass (lb)
		1				**2**				**3**			
-1	0.2651	0.2942	0.0291	0		0.2919	0.0268	0		0.2938	0.0287	0	
0	0.2652	0.2974	0.0322	0	440.5000	0.2959	0.0307	0	438.6000	0.3013	0.0361	0	441.8000
1	0.2651	0.2994	0.0343	0.021	441.1000	0.2968	0.0317	0.01	440.1000	0.3019	0.0368	0.007	442.0000
3	0.2652	0.3005	0.0353	0.031	441.9000	0.2976	0.0324	0.017	440.6000	0.3029	0.0377	0.016	442.8000
5	0.2652	0.3014	0.0362	0.040	442.3000	0.2986	0.0334	0.027	440.9000	0.3036	0.0384	0.023	443.1000
7	0.265	0.3016	0.0366	0.044	442.4000	0.2985	0.0335	0.028	441.0000	0.3036	0.0386	0.025	443.2000
10	0.265	0.3018	0.0368	0.046	443.1000	0.2989	0.0339	0.032	441.9000	0.3039	0.0389	0.028	444.3000
14	0.2648	0.3028	0.038	0.058	443.4000	0.2997	0.0349	0.042	442.1000	0.305	0.0402	0.034	444.2000

Table A5

PC77.5FAF12.5GGBFS10 Ternary Blended Alkali-Silica Reaction

Time (days)	Std Bar RDG (in)	Specimen RDG (in)	CRD	ΔL_x (%)	Mass (lb)	Specimen RDG (in)	CRD	ΔL_x (%)	Mass (lb)	Specimen RDG (in)	CRD	ΔL_x (%)	Mass (lb)
		1				**2**				**3**			
-1	0.2651	0.2958	0.0307	0		0.2986	0.0335	0		0.2958	0.0307	0	
0	0.2652	0.2955	0.0303	0	433.20	0.2931	0.0279	0	440.60	0.2964	0.0312	0	437.20
1	0.2651	0.2961	0.031	0.007	433.90	0.2938	0.0287	0.008	441.00	0.297	0.0319	0.007	437.80
3	0.2652	0.2966	0.0314	0.011	434.70	0.2944	0.0292	0.013	442.00	0.2976	0.0324	0.012	438.50
5	0.2652	0.2972	0.032	0.017	435.10	0.295	0.0298	0.019	442.20	0.2983	0.0331	0.019	438.90
7	0.265	0.2971	0.0321	0.018	435.30	0.295	0.03	0.021	442.60	0.2981	0.0331	0.019	439.20
10	0.265	0.2973	0.0323	0.02	436.10	0.2952	0.0302	0.023	443.00	0.2982	0.0332	0.02	439.90
14	0.2648	0.2982	0.0334	0.031	436.50	0.2962	0.0314	0.035	443.70	0.2991	0.0343	0.031	440.00

Table A6

PC72.5FAC25SF2.5 Ternary Blended Alkali-Silica Reaction

Time (days)	Std Bar RDG (in)	Specimen RDG (in)	CRD	ΔL_x (%)	Mass (lb)	Specimen RDG (in)	CRD	ΔL_x (%)	Mass (lb)	Specimen RDG (in)	CRD	ΔL_x (%)	Mass (lb)
		1				**2**				**3**			
-1	0.2652	0.2948	0.0296	0	438.90	0.2908	0.0256	0	428.20	0.2875	0.0223	0	435.90
0	0.2651	0.2932	0.0281	0	438.60	0.2958	0.0307	0	430.40	0.3005	0.0354	0	441.40
1	0.2653	0.2946	0.0293	0.012	439.20	0.2975	0.0322	0.015	431.10	0.3019	0.0366	0.012	442.00
3	0.2652	0.2957	0.0305	0.024	439.80	0.2984	0.0332	0.025	431.50	0.3028	0.0376	0.022	442.50
5	0.2651	0.2962	0.0311	0.03	440.00	0.2989	0.0338	0.031	431.80	0.3033	0.0382	0.028	442.60
7	0.2651	0.2962	0.0311	0.03	440.00	0.2989	0.0338	0.031	432.00	0.3033	0.0382	0.028	443.30
10	0.2648	0.2966	0.0318	0.037	440.90	0.2993	0.0345	0.038	432.70	0.3037	0.0389	0.035	443.90
14	0.2649	0.2968	0.0319	0.038	441.30	0.2996	0.0347	0.04	433.00	0.3041	0.0392	0.038	444.00

Table A7

Ternary Blended RCA Hardened Properties

	NC	NC30	NC30T	NC50T
Compressive Strength				
3d (psi)	3894	4984	4152	4714
7d (psi)	4700	5351	5069	5662
14d (psi)	5030	5942	5435	6238
28d (psi)	5291	6186	5768	6571
56d (psi)	5943	6740	6125	7316
90d (psi)	6246		6894	7671
Elastic Modulus				
3d (ksi)	7217	7416	7916	8415
7d (ksi)	7910	7798	8828	8983
14d (ksi)	7837	7929	8502	8779
28d (ksi)	8896	8728	8589	8145
56d (ksi)	9854	9361	9455	8515
90d (ksi)	9483		9433	9087
Electrical Resistivity				
3d (kΩ/cm)	7.9	8.4	6.8	6.2
7d (kΩ/cm)	9.9	9.9	9.6	7.9
14d (kΩ/cm)	11.3	12.7	12.1	10.8
28d (kΩ/cm)	13.7	13.5	17.1	14.5
56d (kΩ/cm)	18.0	16.7	22.0	20.2
90d (kΩ/cm)	19.7		27.4	23.7
Modulus of Rupture				
28d (psi)	990	1034	1111	1013
90d (psi)	1045	1089	1108	1107

Table A8

NC Alkali-Silica Reaction

Time (days)	Std Bar RDG (in)	Specimen RDG (in)	CRD	ΔL_x (%)	Mass (g)	Specimen RDG (in)	CRD	ΔL_x (%)	Mass (g)	Specimen RDG (in)	CRD	ΔL_x (%)	Mass (g)
		1				2				3			
-1	0.2348	0.2569	0.0221	0	444.88	0.2563	0.0215	0	440.14	0.2578	0.023	0	443.68
0	0.235	0.2638	0.0288	0	444.6	0.2634	0.0284	0	440.64	0.2649	0.0299	0	444.09
1	0.2347	0.2642	0.0295	0.007	445.29	0.2634	0.0287	0.003	440.63	0.2654	0.0307	0.008	444.3
3	0.2348	0.2645	0.0297	0.009	445.51	0.2637	0.0289	0.005	441.41	0.2657	0.0309	0.01	444.86
5	0.2343	0.2649	0.0306	0.018	445.8	0.2638	0.0295	0.011	441.7	0.2657	0.0314	0.015	444.98
7	0.2349	0.2656	0.0307	0.019	445.5	0.2653	0.0304	0.02	441.28	0.2668	0.0319	0.02	444.84
10	0.2347	0.2665	0.0318	0.03	445.7	0.2659	0.0312	0.028	441.61	0.2671	0.0324	0.025	444.91
14	0.2351	0.2673	0.0322	0.034	445.48	0.2664	0.0313	0.029	441.2	0.268	0.0329	0.03	444.75

Table A9

NC30 Alkali-Silica Reaction

Time (days)	Std Bar RDG (in)	Specimen RDG (in)	CRD	ΔL_x (%)	Mass (g)	Specimen RDG (in)	CRD	ΔL_x (%)	Mass (g)	Specimen RDG (in)	CRD	ΔL_x (%)	Mass (g)
		1				2				3			
-1	0.2348	0.2562	0.0214	0	442.63	0.2592	0.0244	0	440.05	0.257	0.0222	0	437.03
0	0.235	0.263	0.028	0	442.64	0.2661	0.0311	0	440.77	0.2634	0.0284	0	437.8
1	0.2347	0.2635	0.0288	0.008	442.75	0.2665	0.0318	0.007	440.7	0.2641	0.0294	0.010	437.86
3	0.2348	0.2638	0.029	0.010	443.42	0.2673	0.0325	0.014	441.28	0.265	0.0302	0.018	438.5
5	0.2343	0.2642	0.0299	0.019	443.55	0.2678	0.0335	0.024	441.38	0.2657	0.0314	0.030	438.52
7	0.2349	0.2661	0.0312	0.032	443.57	0.2691	0.0342	0.031	441.35	0.2669	0.0320	0.036	438.65
10	0.2347	0.2677	0.033	0.050	444.3	0.271	0.0363	0.052	442.13	0.2672	0.0325	0.041	439.17
14	0.2351	0.2714	0.0363	0.083	444.27	0.2742	0.0391	0.080	442.37	0.2721	0.0370	0.086	439.5

Table A10

NC30T Alkali-Silica Reaction

Time (days)	Std Bar RDG (in)	Specimen RDG (in)	CRD	ΔL_x (%)	Mass (g)	Specimen RDG (in)	CRD	ΔL_x (%)	Mass (g)	Specimen RDG (in)	CRD	ΔL_x (%)	Mass (g)
			1				2				3		
-1	0.2354	0.2607	0.0253	0	439.2	0.2598	0.0244	0	432.1	0.2613	0.0259	0	438
0	0.2355	0.2676	0.0321	0	440.92	0.2661	0.0306	0	433.5	0.2677	0.0322	0	439.79
1	0.2348	0.2692	0.0344	0.023	441.26	0.2678	0.033	0.024	434.26	0.2694	0.0346	0.024	440.46
3	0.2348	0.2696	0.0348	0.027	441.22	0.2688	0.034	0.034	434.63	0.2705	0.0357	0.035	440.71
5	0.2348	0.27	0.0352	0.031	441.94	0.2689	0.0341	0.035	435.02	0.2703	0.0355	0.033	441.07
7	0.2348	0.271	0.0362	0.041	442.25	0.2705	0.0357	0.051	435.46	0.2716	0.0368	0.046	441.64
10	0.2352	0.2728	0.0376	0.055	442.53	0.2722	0.037	0.064	435.61	0.2733	0.0381	0.059	441.87
14	0.235	0.2764	0.0414	0.093	443.71	0.2766	0.0416	0.11	442.7	0.2752	0.0402	0.08	436.63

Table A11

NC50T Alkali-Silica Reaction

Time (days)	Std Bar RDG (in)	Specimen RDG (in)	CRD	ΔL_x (%)	Mass (g)	Specimen RDG (in)	CRD	ΔL_x (%)	Mass (g)
		1				2			
-1	0.2354	0.2589	0.0235	0	431.7	0.2569	0.0215	0	438.6
0	0.2355	0.2649	0.0294	0	433.6	0.2637	0.0282	0	440.5
1	0.2348	0.2662	0.0314	0.02	434.13	0.2651	0.0303	0.021	440.35
3	0.2348	0.2664	0.0316	0.022	434.22	0.2666	0.0318	0.036	440.9
5	0.2348	0.2667	0.0319	0.025	435.9	0.2667	0.0319	0.037	441.55
7	0.2348	0.2689	0.0341	0.047	435.43	0.2684	0.0336	0.054	442.03
10	0.2352	0.2715	0.0363	0.069	435.96	0.2719	0.0367	0.085	442.35
14	0.235	0.2772	0.0422	0.128	436.94	0.277	0.042	0.138	443.19

Table A12

NC50Tb Alkali-Silica Reaction

Time (days)	Std Bar RDG (in)	Specimen RDG (in)	CRD	ΔL_x (%)	Mass (g)	Specimen RDG (in)	CRD	ΔL_x (%)	Mass (g)	Specimen RDG (in)	CRD	ΔL_x (%)	Mass (g)
		1				2				3			
-1	0.2342	0.2598	0.0256	0	446.21	0.2568	0.0226	0	438.14	0.2565	0.0223	0	439.47
0	0.2342	0.2663	0.0321	0	445.3	0.264	0.0298	0	440	0.2639	0.0297	0	442
1	0.2342	0.2673	0.0331	0.01		0.2645	0.0303	0.005			-0.2342	0	
3	0.2342	0.2676	0.0334	0.013		0.2643	0.0301	0.003		0.2645	0.0303	0.006	
5	0.2342	0.2678	0.0336	0.015		0.2651	0.0309	0.011		0.2646	0.0304	0.007	
7	0.2342	0.2689	0.0347	0.026	449.4	0.2658	0.0316	0.018	441.9	0.2654	0.0312	0.015	443.7
10	0.2342	0.2692	0.035	0.029	449.8	0.2663	0.0321	0.023	442.5	0.2656	0.0314	0.017	444.1
14	0.2348	0.2717	0.0369	0.048	451	0.2686	0.0338	0.04	443	0.2683	0.0335	0.038	444